Bifidobacterium longum modifies a nutritional intervention for stunting in Zimbabwean infants

Authors: Ethan K Gough[1,*], Thaddeus J Edens[2], Lynnea Carr[3], Ruairi C Robertson[4], Kuda Mutasa[5], Robert Ntozini[5], Bernard Chasekwa[5], Hyun Min Geum[6], Iman Baharmand[6], Sandeep K Gill[6], Batsirai Mutasa[5], Mduduzi N N Mbuya[5,7], Florence D Majo[5], Naume Tavengwa[5], Freddy Francis[8], Joice Tome[5], Ceri Evans[4], Margaret Kosek[9], Jean H Humphrey[1,5], Andrew J Prendergast[4,5], Amee R Manges[6,10] for the Sanitation Hygiene Infant Nutrition Efficacy (SHINE) Trial Team.

Affiliations:

1. Department of International Health, Johns Hopkins Bloomberg School of Public Health, Baltimore, MD, 21205, USA.
2. Devil's Staircase Consulting, West Vancouver, BC, Canada.
3. Department of Microbiology and Immunology, University of British Columbia, Vancouver, BC, V6T 1Z3, Canada.
4. Blizard Institute, Queen Mary University of London, London, E1 2AT, UK.
5. Zvitambo Institute for Maternal and Child Health Research, Harare, Zimbabwe.
6. School of Population and Public Health, University of British Columbia, Vancouver, BC, V6T 1Z3, Canada.
7. Global Alliance for Improved Nutrition, Washington, DC, 20036, USA.
8. Department of Experimental Medicine, University of British Columbia, Vancouver, BC, V6T 1Z2, Canada.
9. University of Virginia, School of Medicine, Charlottesville, VA, USA.
10. British Columbia Centre for Disease Control (BCCDC), Vancouver, BC, Canada.

*Correspondence: egough1@jh.edu

Summary (word limit: 150)

Child stunting is an indicator of chronic undernutrition and reduced human capital. However, it remains a poorly understood public health problem. Small-quantity lipid-based nutrient supplements (SQ-LNS) have been widely tested to reduce stunting, but have modest effects. The infant intestinal microbiome may contribute to stunting, and is partly shaped by mother and infant histo-blood group antigens (HBGA). We investigated whether mother-infant fucosyltransferase status, which governs HBGA, and the infant gut microbiome modified the impact of SQ-LNS on stunting at age 18 months among Zimbabwean infants in the SHINE Trial (NCT01824940). We found that mother-infant fucosyltransferase discordance and *Bifidobacterium longum* reduced SQ-LNS efficacy. Infant age-related microbiome shifts in *B. longum* subspecies dominance from *infantis*, a proficient human milk oligosaccharide utilizer, to *suis* or *longum*, proficient plant-polysaccharide utilizers, were partly influenced by discordance in mother-infant FUT2+/FUT3- phenotype, suggesting that a "younger" microbiome at initiation of SQ-LNS reduces its benefits on stunting.

Keywords: microbiome, nutrition, fucoslytransferase, histo-blood group antigen, stunting, infant

Introduction

Globally, 21% of children under 5 years of age (149 million) are stunted[1], defined as having a length or height >2 standard deviations below an age- and sex-matched reference population median[2]. Deficits in linear growth largely accrue from conception to 24 months of age[3,4], corresponding to the period when normal child growth and development is most rapid. Stunting is associated with reductions in child survival, neurodevelopment, educational attainment, and adult economic productivity[5–7].

A broadly tested intervention to reduce stunting has been provision of small-quantity lipid-based nutrient supplements (SQ-LNS) to improve infant and young child feeding (IYCF) starting at 6-months (mo) of age, which is the recommended time for introduction of complementary foods. Randomized controlled trials (RCT) of SQ-LNS provision to infants have shown small reductions in stunting (12% relative reduction), but effects have varied[8,9]. Evidence to support other nutrition interventions, which address the underlying determinants of stunting during the first 1000 days of life, starting from conception, is also limited[10]. Elucidating the reasons for the limited impact of nutritional interventions that are designed to alleviate stunting is crucial to the development of more effective strategies.

Recently, the human microbiome has been shown to impact infant health[11], and studies suggest a role of the intestinal microbiome in child growth, particularly ponderal growth[12,13]. The prevailing view holds that intestinal colonization with bacteria begins at birth, after which the microbiome progresses through a succession of identifiable shifts in composition and functional capacity[11] that correspond closely with infant age and developmental stage[14]. Deviations from an age-appropriate composition may be associated with poor health outcomes[14–17], including undernutrition in low resource settings[14,18–20]. However, results vary[21–25] and evidence for a causal effect of the intestinal microbiome on growth comes predominantly from animal models. In these experiments, a combination of commensal bacteria and a nutrient-poor diet produce a synergistic effect on growth faltering. The detrimental effect on growth was worse when certain commensal bacteria, which can act as opportunistic pathogens (e.g.

Bacteroides thetaiotaomicron and *Bacteroides fragilis*), were present in the gut along with pathogenic species[26,27].

The gut microbiome in infants is influenced by breastfeeding, with differences persisting beyond age 6mo[16]. Breastfeeding-associated differences are partly driven by differences in human milk oligosaccharide (HMO) composition, which are metabolized by specific commensal bacteria and thereby influence the growth and activity of specific bacterial populations in the infant gut, in particular, Bifidobacterium[28,29]. In addition, HMOs in combination with commensal gut bacteria have been shown to improve growth in animal models of undernutrition[30]. Active maternal α-1,2-fucosyltransferase (FUT2) and α-1,3-fucosyltransferase (FUT3) genes are key determinants of HMO composition[31–33]. These genes encode enzymes which catalyze addition of fucose to the disaccharides that serve as precursors to host glycan production[34,35]. Individuals with at least one functional FUT2 or FUT3 allele produce fucosylated histo-blood group antigens (HBGA) and are called “secretors” or “Lewis-positive”, respectively;[35] by contrast, individuals lacking two functional FUT2 or FUT3 alleles don’t produce fucosylated HBGAs, and are termed “non-secretors” or “Lewis-null”, respectively[35]. These secretor and Lewis phenotypes act in concert to synthesize a variety of HBGAs (Figure S1)[34,35]. In addition to the impact of maternal FUT2 or FUT3 status on the infant gut microbiome via their influence on HMO composition, host FUT2 and FUT3 phenotypes also determine tissue surface HBGA expression in the gut, which may also affect the microbiome through the availability host glycans and competition for adhesion sites[36–40].

There is growing interest in the moderating effect of the gut microbiome on nutritional interventions. Recent RCTs showed that the impact of dietary interventions for weight-reduction on metabolic health outcomes is modified up to 4-fold by microbiota composition[41–44]. Effect modification of host diet by the gut microbiota has also been investigated in observational studies, which report that microbiome composition modified the association between diet and biomarkers of metabolic syndrome

by up to 2-fold[45–47]. Gut microbiota composition, therefore, may also be an important modifier of dietary interventions on infant health. Only one study to date investigated the gut microbiota as an effect modifier of SQ-LNS on infant stunting, and reported limited evidence of effect-modification[48]. However, several studies have reported a synergistic effect of microbiome composition and diet on undernutrition phenotypes using animal models[26,27,49,50].

Here we aimed to determine the effect of infant gut microbiome composition and functional capacity on efficacy of an IYCF intervention that included SQ-LNS to reduce stunting (primary outcome) and improve length-for-age z-score (LAZ) (secondary outcome) at age 18mo. We hypothesized that the efficacy of IYCF, when started at age 6mo, on infant linear growth is modified by mother and infant FUT2 and FUT3 phenotype, as an early driver of variation in gut microbiome composition, and by the infant gut microbiome. We tested this hypothesis using data from HIV-unexposed infants enrolled in the Sanitation Hygiene Infant Nutrition Efficacy (SHINE) trial conducted in rural Zimbabwe, in which the IYCF intervention modestly increased LAZ by 0.16 standard deviations and reduced stunting by 20% at age 18mo[51]. We found that mother-infant FUT2 and FUT3 phenotype was associated with reduced IYCF impact on stunting at 18mo. Reduced impact of IYCF on stunting was also associated with age-related changes in infant microbiome species composition, characterized by a shift away from *Bifidobacterium longum* carriage. *B. longum*-dominant microbiome composition was characterized by *B. longum* strains that were most similar to subspecies *infantis*, a proficient HMO utilizer. In addition, *B. longum* abundance and odds of detecting different *B. longum* strains were explained by infant age and mother-infant FUT2 and FUT3 phenotype.

Results

Mother-infant FUT2+/FUT3- phenotype discordance modifies the effect of IYCF on stunting at 18mo

In a substudy of the SHINE trial, we assessed FUT2 and FUT3 status in mothers and infants from saliva samples[54]. In order to determine the impact of maternal and infant HBGA on IYCF efficacy, we investigated whether concordance in secretor (FUT2) and Lewis (FUT3) phenotypes between mother and infant pairs modified the effect of IYCF on stunting or LAZ at 18mo. We also used combinations of FUT2 and FUT3 status (Table S1) in order to more precisely reflect the potential for joint activity of these enzymes in HBGA production on linear growth (Figure S1). Paired mother-infant FUT2/FUT3 phenotypes were classified as *both* (if mother and infant shared the same phenotype), *none* (if neither had the phenotype), *infant only* (if the infant had the phenotype but the mother did not) or *mother only* (if the infant did not have the phenotype but the mother did). We fitted multivariable regression models that included interaction terms for IYCF-by-paired mother-infant FUT2/FUT3 phenotype combinations, as well as prespecified covariates from the 6mo follow-up visit when IYCF was started, with stunting status at the 18mo visit as the dependent variable. We fitted separate models for each FUT2/FUT3 phenotype combination (Table S1, Figure S1). These models were restricted to 792 infants who had both maternal and infant FUT2 and FUT3 status ascertained (Figure S2). Analyses were repeated with LAZ at the 18mo visit as the dependent variable.

Amongst infants who were randomized to IYCF, those who were in the *mother only* FUT2+/FUT3- group (13.5%), had a probability of stunting at 18mo that was -33.0% lower (95%CI:-55.0%,-10.0%) than infants in the *both* FUT2+/FUT3- group (11.1%) (Table 1). The *infant only* (11.1%) and *none* (64.3%) FUT2+/FUT3- groups and other mother-infant FUT2 and FUT3 phenotype combinations (Table S1, Figure S1) did not show evidence of effect modification of IYCF on stunting (Table S2), and there was no evidence of effect modification on LAZ at 18mo after FDR-adjustment for multiple testing (Table S3). Overall, our results indicate that discordance between mothers and infants in the FUT2+/FUT3-

phenotype, whereby mothers had the phenotype and infants didn't have the phenotype, was associated with increased efficacy of IYCF to reduce stunting but not to increase LAZ.

Infant gut microbiome composition modifies the effect of the IYCF intervention on stunting at 18mo

Given our finding that infants whose mothers were FUT2+/FUT3-, while the infant was not, had greater reductions in stunting by IYCF; and considering the potential importance of FUT2/FUT3 phenotypes on early infant microbiome composition via variation in maternal HMO composition and infant gut epithelial HBGA expression, we investigated whether infant gut microbiota species turnover showed evidence for modification of IYCF efficacy on stunting or LAZ at 18mo. First, we used 354 infant metagenomes from 172 infants collected from 1-18mo of age to fit a constrained Principal Coordinates Analysis (PCoA) model that included infant age at stool collection and three dummy variables for mother-infant FUT2+/FUT3- status representing the *none*, *infant only*, and *mother only* groups with the *both* group as the referent (see next section for details). Thus, we derived four PCoA axis scores from this model representing variation in microbiome composition due to infant age and *none*, *infant only*, or *mother only* FUT2+/FUT3- status compared to *both*. Next, we fitted a multivariable regression model that included an IYCF-by-PCoA axis 1 score interaction term and prespecified covariates. The regression model was restricted to 53 infants who had a fecal specimen collected at the 6mo follow-up visit when IYCF started and used their covariate values at the 6mo visit (Figure S2), and stunting status at 18mo was used as the dependent variable. We repeated our analyses using PCoA axis 2 to 4 scores. Finally, we fitted regression models replacing stunting status with LAZ at 18mo as the dependent variable.

Greater PCoA axis 1 scores represented species turnover with increasing infant age (Figure S3), while greater PCoA axis 2 scores represented changes in species composition associated with mother-infant FUT2+/FUT3- phenotypes (Figure S3). PCoA axis 1 and 2 scores showed evidence of interaction with IYCF on stunting at 18mo (Table 2), but not LAZ (Table S4). Amongst infants randomized to IYCF, those with

higher PCoA axis 1 scores at age 6mo were less likely to be stunted at 18mo compared to infants with lower PCoA axis 1 scores (difference-in-differences -76.0%[95%CI: -99.0%,-32.0%, adjusted p=0.003) (Table 2). In contrast, infants randomized to IYCF with higher PCoA axis 2 scores at age 6mo were more likely to be stunted at 18mo compared to infants who had lower PCoA axis 2 scores (difference-in-differences, 14.0%[95%CI: 7.0%,21.0%], adjusted p=0.001) (Table 2). Taken together, our findings showed that infant age-related microbiome species turnover was associated with greater reduction in the probability of stunting at 18mo by IYCF, indicating greater efficacy of the intervention; while microbiome species composition related to mother-infant FUT2+/FUT3- phenotype was associated with lesser reduction in stunting, suggesting variation in microbiome composition due to these infant characteristics is an important determinant of SQ-LNS efficacy to reduce stunting.

Infant age and mother-infant FUT2+/FUT3- phenotype explain microbiome species turnover, in particular, Bifidobacterium longum

To investigate sources of variation in infant intestinal microbiome composition and derive interpretable measures of species turnover, we performed constrained PCoA of Bray-Curtis dissimilarities with permutational analysis of variance using distance matrices for hypothesis testing. Infant age at stool collection explained 12.6% (ADONIS2 p=0.001) of the variability in microbiome composition (Table S5). Notably, exclusive breastfeeding (EBF) at 3mo was not significantly associated (R^2=0.346, ADONIS2 p=0.483) with microbiome composition (Table S5). However, 93.2% of mothers in these analyses reported exclusive breastfeeding (Table S6). Thus, there may not have been sufficient variability in infant breastfeeding practices in this cohort to identify EBF-associated differences between infant microbiomes. Also, inclusion of specimens collected throughout the follow-up period in our PCoA models may have obscured associations with EBF, since EBF is only recommended up to age 6mo.

We then fitted a fully adjusted multivariable constrained PCoA model that included both infant age at stool collection and mother-infant FUT2+/FUT3- phenotype. We retained the latter variable to capture variation in microbiota composition associated with mother-infant FUT2/FUT3 status after controlling for infant age, because of our *a priori* aim to investigate whether microbiome variation due to mother and infant FUT2/FUT3 phenotype was a modifier of the IYCF intervention, and our finding that the *mother only* FUT2+/FUT3- group was associated with a modified intervention effect. In the full model, age explained 12.8% (ADONIS p=0.001) and mother-infant FUT2+/FUT3- phenotype explained 0.81% (ADONIS p=0.323) of the variance in microbiome composition (Table S5), indicating that infant age was the main driver of microbiome-wide species-turnover in this cohort.

Age-related species turnover was characterized by decreased relative abundance of *B. longum*, and increased relative abundance of *Prevotella copri*, *Faecalibacterium prausnitzii*, *Dorea longicatena*, and *Dorea formicigenerans* (Figure S4). Mother-infant FUT2+/FUT3- discordance was characterized by increased relative abundance of *B. longum* in the *none* and *infant only* groups (Figure S5-S7).

In combination with our IYCF-by-PCoA effect modification models (see previous section), these findings indicate that infant age-associated species turnover characterized by a shift away from a microbiome dominated by *B. longum* (i.e. greater PCoA axis 1 score) was associated with a reduction in the probability of stunting at age 18mo in infants randomized to IYCF (Table 2). In contrast, species composition associated with mother-infant FUT2+/FUT3- phenotype (i.e. greater PCoA axis 2 score), which was characterized by higher *B. longum* abundance, showed evidence of reduced impact of IYCF on stunting (Table 2).

Bifidobacterium longum relative abundance modifies the effect of the IYCF intervention on stunting at 18mo

To determine if differences in the relative abundances of specific microbiome species that characterized the constrained PCoA axes were also associated with significant modification of IYCF on stunting or LAZ at 18mo, we fitted multivariable regression models that included IYCF-by-species relative abundance interaction terms and prespecified covariates as described in the previous sections. These models were restricted to 53 infants who had a fecal specimen collected at the 6mo follow-up visit when IYCF started and used their covariate values at that visit (Figure S2). We fitted a separate model for each microbiome species of interest. Infants randomized to IYCF who had greater relative abundance of *B. longum* when the intervention started were more likely to be stunted at age 18mo compared to infants with lower relative abundance of *B. longum* (differences-in-differences 50.0%[95%CI: 26.0%,74.0%], adjusted p<0.001) (Table 3). No other species-level interactions with IYCF on stunting were identified (Table 3). Infants randomized to IYCF with greater *B. longum* relative abundance also had smaller LAZ at 18mo compared to infants with lower *B. longum* abundance; however, this association was not statistically significant after FDR-adjustment (differences-in-differences -0.88[95%CI: -1.45,-0.31], adjusted p=0.074) (Table S7). Overall, our findings indicate that greater relative abundance of *B. longum* in the infant gut microbiome at initiation of the IYCF intervention was associated with less efficacy of the IYCF intervention to reduce stunting at age 18mo.

Infants randomized to IYCF in the mother only FUT2+/FUT3- group or with lower B. longum relative abundance were spared from more severe growth faltering

To investigate whether these reductions in IYCF efficacy were due to differences in the degree or timing of growth faltering, we plotted (i) LAZ growth trajectories and (ii) LAZ velocities (sd/mo) from 6-18mo of age, by both IYCF arm and paired mother-infant FUT2+/FUT3- phenotype. Infants randomized to IYCF in the *mother only* group had a less steep decline in LAZ trajectories on average compared to infants in the *mother only* group randomized to no IYCF (Figure 1). In addition, although all groups of

235 infants had negative 6-18mo LAZ velocities on average, infants in the *mother only* group who were
236 randomized to IYCF had higher LAZ velocity on average (-0.02 sd/mo,95%CI[-0.05,0.00]) compared to
237 those in the no IYCF group (-0.08 sd/mo, 95%CI[-0.11,-0.05]) (Figure 1). Importantly, infants in the
238 *mother only* group also benefitted more from the IYCF intervention in our interaction models (Table 1).
239 We repeated these exploratory analyses to compare LAZ trajectories and LAZ velocities by both IYCF
240 arm and *B. longum* at the 6mo visit stratified above or below the relative abundance median. Infants
241 randomized to IYCF who were above the median relative abundance of *B. longum* had declining growth
242 trajectories on average, while infants below the median did not (Figure 2). Furthermore, the mean 6-
243 18mo LAZ velocity was negative in both *B. longum* groups, but trended toward being higher in the group
244 with relative abundance below (-0.02 sd/mo,95%CI[-0.07,0.03]) compared to above (-0.08 sd/mo
245 95%CI[-0.12,-0.03]) the median; however, the 95% confidence intervals overlapped. In contrast, among
246 infants randomized to no IYCF, both those with a relative abundance above and those with a relative
247 abundance below the median at the 6mo visit had declining growth trajectories (Figure 2) with similar
248 average negative LAZ velocities (Figure 2).
249 Overall, these results indicate that the differences in IYCF efficacy by mother-infant FUT2+/FUT3-
250 phenotype and *B. longum* relative abundance can be explained by differences in LAZ velocity. Infants in
251 the *mother only* FUT2+/FUT3- group and infants with lower *B. longum* relative abundance at 6mo were
252 spared from more severe LAZ declines, which contributed to a lower probability of stunting at 18mo,
253 even when the differences in velocity were not statistically significant.
254
255 *Bifidobacterium longum strains most similar to subspecies infantis dominate the early infant gut*
256 *microbiome*
257 Next, we aimed to identify whether infants carried different strains of *B. longum* using a pangenome
258 approach. We used PanPhlan3.0[52] to generate UniProt gene family profiles of dominant *B. longum*

strains from 218 infant gut metagenomes, generated from 136 infant, with sufficient coverage of *B .longum* (Figure S2). To assess similarities between SHINE *B. longum* strains and previously characterized subspecies, we also included UniProt gene family profiles produced by PanPhlan for 118 reference strains. We performed PCoA using Jaccard dissimilarities calculated from these gene family presence or absence profiles. Three clusters of *B. longum* strains were identifiable by visualization of ordination plots (Figure 3 and S8). We, therefore, performed hierarchical clustering of these Jaccard dissimilarities to delineate three distinct strain clusters and place each strain into the most appropriate cluster (Figure S8). Subspecies *infantis* reference strains predominantly grouped with the largest cluster of strains (hereafter called the *infantis* cluster) and included 15 *infantis* reference strains and 255 SHINE strains (Figure 3). Subspecies *longum* reference strains predominantly grouped with the second largest cluster of strains (*longum* cluster), including 29 *longum*, 3 *infantis*, 64 *unclassified* subspecies strains and 14 SHINE strains. The remaining cluster included two subspecies *suis*, one subspecies *longum*, 4 *unclassified* subspecies reference strains and 15 SHINE strains (*suis* cluster) (Figure 3 and Figure S8).

The infant gut microbiome undergoes a transition with age in which Bifidobacterium longum strains most similar to subspecies infantis become less prevalent

To investigate predictors of *B. longum* relative abundance in infants over time, we fitted a longitudinal multivariable zero-inflated mixed-effects model, using 225 specimens from 87 infants with prespecified, non-missing covariate data. Covariates included infant age at specimen collection, sex, EBF at 3mo, minimum infant dietary diversity at specimen collection, and mother-infant FUT2+/FUT3- phenotypes (Figure S2). Infant age and mother-infant FUT2+/FUT3- phenotype were significant predictors of *B. longum* relative abundance. Each one month increase in infant age was associated with a 0.91-fold decrease (95%CI:0.90,0.92, $p<0.001$) in *B. longum*, and the *mother only* FUT2+/FUT3- group

had the lowest relative abundance of *B. longum* throughout follow-up (Figure S11) with a 0.71-fold decrease in relative abundance (95%CI:0.59,0.87, p=0.001) relative to the *both* group (Table S9).

Also, to determine predictors of *B. longum* strain cluster detection in infants over time, we fitted multivariable longitudinal logistic regression models using 133 specimens from 70 infants with PanPhlan3.0 output and prespecified, non-missing covariate data (Figure S2). We fitted a separate model for each strain to estimate its probability of detection. Results were consistent with predictors of *B. longum* relative abundance. Each one month increase in infant age was associated with a 0.85-fold decreased odds (95%CI:0.75,0.96, p=0.008) of the *infantis* cluster (Table S10). At the same time, the *suis* and *longum* clusters increased with age (Table S10 & Figure S12). Female infants had 8.35-fold increased odds (95%CI:3.17,21.97, p<0.001), and the *infant only* FUT2+/FUT3- group, which had the highest probability of the *infantis* cluster throughout follow-up (Figure S13A), had a 4.66-fold increased odds (95%CI:1.05,20.71, p=0.043) of the *infantis* cluster (Table S10). In contrast, the *mother only* FUT2+/FUT3- group had low probability of carrying an *infantis* cluster strain (Figure S13A & Table S10) and the highest probability of carrying a *suis* cluster strain (Figure S13C).

In summary, *B. longum* decreased with infant age and was lowest among infants in the *mother only* FUT2+/FUT3- group. The *infantis* cluster, which included the dominant *B. longum* strains, also decreased with infant age. Furthermore, *infantis* cluster strains were most likely to be detected in the *infant only* group, and less likely to be detected in the *mother only* group which were more likely to carry *suis* cluster strains. Infant age and mother-infant FUT2+/FUT3- phenotype were important determinants of both *B. longum* relative abundance and strain carriage.

Bifidobacterium longum strains most similar to subspecies infantis were characterized by greater capacity for HMO degradation, uptake, siderophore and antimicrobial biosynthesis

To identify differences in metabolic potential between *B. longum* strain clusters, we used two-sided Fisher's Exact tests to compare UniProt gene family presence between clusters. We restricted these analyses to the 284 SHINE *Bifidobacterium* pangenomes in order to make inferences about differences in metabolic potential between SHINE strains. We then performed overrepresentation analyses[53] of differentially frequent gene families by one-sided Fisher's Exact test to determine whether they were more likely to be involved in specific GO biological processes[54], or to function as specific carbohydrate-active enzymes (CAZymes)[55] or transporters[56]. Gene families that were more common in the *infantis* cluster were more likely to be involved in HMO degradation, and included genes that function as CAZyme Glycoside Hydrolase Family 20 (GH20) (β-N-acetylglucosaminidases, β-N-acetylgalactosamindase, β-6-SO3-N-acetylglucosaminidases, and lacto-N-biosidases), GH29 (fucosidases), GH95 (fucosidases), and GH33 (sialidases) (Figure 4A, Table S8). Conversely, gene families that were more common in the other clusters were more likely to be involved in degradation of plant-derived polysaccharides, including genes that function as GH42 (β-galactosidases), GH51 (L-arabinfuranosidases) and GH127 (β-L-arabinofuranosidase) CAZymes (Figure 4A, Table S8). Similarly, gene families that were more common in the *infantis* cluster were more likely to function as transporters involved in oligosaccharide uptake (TCID 3.A.1.1.59), while those that were less common in the *infantis* cluster were more likely to be involved in uptake of fructose and other sugars (TCID 3.A.1.2.23) (Figure 4A, Table S8). Other differences between strain clusters included greater carriage of gene families among *infantis* cluster strains that are involved in riboflavin biosynthesis, signal transduction, amino acid catabolism and uptake.

We also identified differences between strain clusters in the frequency of 115 MetaCyc[57] pathways identified using MinPath[58] (Figure S10). Pathways that were more common in the *infantis* cluster were more likely to be involved in generation of precursor metabolites and energy, and secondary metabolite biosynthesis (which predominantly included pathways for biosynthesis of siderophores and

329 antimicrobials) (Figure 4B, Table S8). Conversely, the *infantis* clusters was less likely to include pathways
330 involved in glycan metabolism and polymeric compound degradation (e.g. pectin, xylan, and
331 arabinogalactan degradation pathways), and in fatty acid and lipid biosynthesis (Figure 4B, Table S8).
332 Overall, infant gut microbiomes were dominated by *B. longum* strains that were most similar to
333 subspecies *infantis* in their UniProt gene family profiles. The primary distinction of *B. longum* strains in
334 the *infantis* cluster was greater capacity for HMO degradation and uptake of oligosaccharides than
335 plant-derived polysaccharides. However, strains in the *infantis* cluster also had greater capacity for
336 siderophore and antimicrobial production, and displayed differences in their capacity for riboflavin, fatty
337 acid, and lipid metabolism.
338
339 **Discussion**

340 In this study of HIV-unexposed infants enrolled in the SHINE trial in rural Zimbabwe, we tested the
341 hypothesis that mother-infant FUT2/FUT3 phenotype and infant gut microbiome modify the effect of an
342 intervention containing small-quantity lipid based nutrient supplements, on infant stunting and LAZ at
343 18mo of age. Our goal was to define mechanisms that explain the rather modest effects of SQ-LNS on
344 linear growth, reasoning that maternal-infant HBGA phenotypes might be important given their
345 combined role in shaping the early-life microbiome. We found that the following features were
346 associated with reduced IYCF impact on stunting at 18mo: (i) discordance in mother-infant FUT2+/FUT3-
347 phenotype, where the mother has the phenotype but the infant does not; (ii) changes in microbiome
348 species composition that reflected a shift from a *B. longum*-dominant microbiome to a microbiome with
349 less *B. longum* and a greater abundance of species characteristic of older infants; and (iii) differences in
350 *B. longum* abundance that were also associated with FUT+/FUT3- status. These findings suggest that a
351 persistently "younger" microbiome, characterized by a high abundance of *B. longum* and carriage of *B.*
352 *longum* strains best suited to HMO metabolism, at the point when complementary foods are introduced

353 into the infant diet, may reduce the beneficial effects of an intervention that includes SQ-LNS on infant
354 stunting.

355 The *mother only* FUT2+/FUT3- group showed evidence of a greater reduction in stunting following
356 receipt of one year of the IYCF intervention. Mother-infant FUT2+/FUT3- phenotype was also a
357 significant predictor of *B. longum*, whereby relative abundance was lower throughout follow-up in the
358 *mother only* group. Active maternal FUT2/FUT3 genes are key determinants of milk oligosaccharide
359 composition[31–33]. Human milk specimens form distinct groups based on maternal FUT2[59] and FUT3
360 phenotype[31,33] by principal component analyses of oligosaccharide composition. In particular,
361 FUT2+/FUT3- mothers are a subset of FUT2+ women who form an HMO cluster that is distinct from
362 mothers with other phenotypes, including FUT2+ mothers who are also FUT3+[31,33]. Differences in HMO
363 composition influence growth and activity of Bifidobacterium populations in the infant gut[28,59]. FUT2
364 status may also affect infant gut microbiome composition[36–40]. Gut Bifidobacterium[39], Bacteroides[36,38],
365 Faecalibacterium[40] and Roseburia[40] are differentially abundant in FUT2+ compared to FUT2- individuals.
366 However, reported differences in microbiome composition by FUT2/FUT3 status have been inconsistent,
367 potentially due to variability in age, dietary patterns, host health, sampled gut sections and
368 methodology between studies[60,614], and studies predominantly include from adults. However, CAZymes
369 found in *B. longum* species that function in HMO degradation (GH29 and GH95) have also been found to
370 function in host intestinal glycan degradation in infants[62]. The evidence, therefore, suggests that the
371 FUT2/FUT3 phenotypes of mother and infant, together, can elicit a strong prebiotic selective pressure,
372 driven by maternal milk and infant glycan composition[28] that influences Bifidobacteria and broader gut
373 microbiota composition in infants.

374 In contrast to our finding that mother-infant FUT2+/FUT3- phenotype predicted the presence of *B.*
375 *longum* subspecies *infantis* cluster strains, a prior study reported that maternal or infant FUT2 or FUT3
376 status did not predict the abundance subspecies *infantis* or *longum* in children[63]. However, we included

infant age as a covariate in our models, while the prior study did not[63]. In addition, to accommodate the fact that FUT2 and FUT3 work in concert biologically to produce different HBGAs and HMOs, we defined combined FUT2 and FUT3 phenotypes (Figure S1). Furthermore, we considered paired maternal and infant phenotypes[63]. Another smaller study found infants born to FUT2+/FUT3- mothers had lower bifidobacterial operational taxonomic unit diversity compared to other infants[39]. This study provides additional evidence that maternal FUT2+/FUT3- phenotype is associated with bifidobacterial taxon composition in the infant gut. Further research is needed to clarify the roles of mother-infant FUT2/FUT3, maternal HMO and the infant glycobiome in driving infant gut microbiome composition and development.

In our PCoA model, infant age-related species turnover predominantly reflected decreased abundance of *B. longum* and increased abundance of *P. copri*, *F. prausnitzii*, *D. longicatena*, and *D. formicigenerans*. These species were also important predictors of infant age in a microbiome-age model previously developed from this same cohort[64]. Age-discriminatory taxa in the same genera were also identified in previously reported microbiome-age models[14]. Delayed gut microbiota-age has been reported in children with severe acute malnutrition (SAM), while improvements in microbiota-age and relative abundance of age-discriminatory taxa have been correlated with better growth[14]. Our analyses complement this literature with evidence that infant age-related species turnover in the gut microbiome increased the effect of the IYCF intervention on stunting at 18mo, while greater relative abundance of *B. longum*, an age-discriminatory taxon which is associated with younger age, reduced the effect. This suggests that delayed maturation of the gut microbiome at the point when complementary foods are introduced and IYCF is initiated, may impair IYCF-induced effects on growth.

Infant age was the strongest determinant of *B. longum* relative abundance over time. This is consistent with previous reports[65]. In breastfed infants, Bifidobacteria are the most abundant gut bacteria[65,66]. Human breast milk is rich in oligosaccharides, which Bifidobacteria preferentially utilize[67].

At introduction of solid foods, a wider variety of nutrients and reduced availability of HMOs correspond to an increase in microbiota diversity, a decrease in Bifidobacterium,[68] greater bacterial diversity, evenness and development of a more adult-like composition by 2–3 years of age[11,69–71].

Utilization of HMOs by Bifidobacterium varies between species and strains[72–78]. We identified three clusters of dominant *B. longum* strains that also varied by infant age and mother-infant FUT2+/FUT3- phenotype. The cluster of strains with pangenomes most similar to subspecies *infantis* had the highest prevalence in early infancy. However, by age 18mo there was a marked decrease in detection of *infantis* cluster strains and a corresponding increase in detection of strains with pangenomes most similar to subspecies *suis,* which had the highest prevalence at 18mo. Strains most similar to subspecies *longum* increased more slowly. This finding is consistent with a recent study that also reported a pattern of succession among three distinct gut *B. longum* clades from birth to 24mo of age. Subspecies *infantis* was dominant in early infancy but peaked at age 6mo and decreased considerably thereafter. While a transitional clade that included strains most similar to subspecies *suis* and *suillum* showed a corresponding increase in abundance that peaked by 18mo, and subspecies *longum* expanded from 15mo-24mo of age[79]. In that report, the transitional *suis/suillum* clade harbored functional capacity to degrade both HMOs and dietary polysaccharides, suggesting it may be an adaptation of the infant gut microbiome to a period when breastfeeding may co-occur with introduction of complementary foods[79]. We add to this work by showing that differences between mother and infant in FUT2+/FUT3- phenotype may also play a role in driving this transition, whereby, throughout follow-up, the *mother only* FUT2+/FUT3- group had a low prevalence of the *infantis* cluster and the highest prevalence of the *suis* cluster; while the *infantis* cluster was most prevalent in the *infant only* group.

B. longum subspecies *infantis* are particularly well adapted for HMO utilization[80,81]. *B. longum* subspecies *longum*, on the other hand, do not grow as well on HMO, and are more specialized for utilization of diet-derived polysaccharides[82]. In our analyses, UniProt gene families that were more

425 frequent in the *infantis* cluster were more likely to be involved in HMO degradation and uptake. Two of
426 CAZyme families more likely to be carried by the *infantis* cluster (GH29[83] and GH33[74]) were previously
427 reported as more prevalent in subspecies *infantis* strains. In contrast, UniProt gene families that were
428 less frequent in the *infantis* cluster were more likely to be involved in uptake of fructose and other
429 simple sugars, including the sugar transporter 3.A.1.2.23, which was previously described in a different
430 *B. longum* subspecies[84]. Furthermore, strains in the *suis* and *longum* clusters were more likely to carry
431 UniProt gene families involved in such MetaCyc pathways as pectin, xylan, and arabinogalactan
432 degradation. UniProt gene families found more frequently in *infantis* cluster strains were also more
433 likely to be involved in siderophore and antimicrobial biosynthesis. Heavy metals such as iron and zinc
434 are essential minerals for nearly all bacteria and their mammalian hosts. Strategies utilized by bacteria
435 to acquire heavy metals include siderophore biosynthesis. Siderophores are low molecular weight iron-
436 chelating compounds that are synthesized by bacteria to scavenge iron and other essential metals such
437 as zinc under nutrient-restricted conditions[85]. For example, Bifidobacterium species isolated from iron-
438 deficient children efficiently sequester iron via siderophore production[86]. Siderophores may provide a
439 competitive advantage to Bifidobacteria[87], which along with antimicrobial biosynthesis[88], may also help
440 protect the infant gut from enteric pathogens that require essential metals for colonization. However,
441 essential metals such as iron and zinc are key components in SQ-LNS formulations[89–91], and produce
442 improvements in linear growth and reductions in stunting risk[92,936]. While siderophore activity varies
443 considerably between Bifidobacterium species and strains, no research to date has investigated
444 sequestration of essential metals by subspecies *infantis* strains commonly found in resource-limited
445 settings. Our analyses suggest that greater abundance of *B. longum*, at the time when IYCF is started,
446 characterized by a predominance of strains with carriage of gene families which confer greater capacity
447 for HMO utilization and siderophore biosynthesis, is associated with reduced impact on stunting at
448 18mo. These suggests potential mechanisms by which a “younger” microbiome can constrain the

beneficial effects of an SQ-LNS intervention on infant stunting. However, more research is required to fully elucidate the biological mechanisms and downstream pathways to stunting that may be involved.

Our results are in contrast to a previous RCT that investigated infant microbiome composition as a modifier of SQ-LNS impact on infant growth In Malawi[48]. However, in the primary analyses of that RCT, there was no effect of SQ-LNS on linear infant growth[94]. Furthermore, SQ-LNS was provided to both mothers during pregnancy and infants starting at 6mo postpartum, active control interventions (iron-folate or multiple micronutrient supplements) were provided to mothers[48,94], and 16S rRNA gene amplification and sequencing were used which can affect taxon detection (including Bifidobacterium) results[95]. A second RCT reported evidence for effect modification of iron supplementation on growth by maternal FUT2 status, where infants of FUT2- mothers randomized to iron supplementation showed greater declines in LAZ than infants of FUT2+ mothers[96]. In addition, a third, recent RCT found that suppression of *B. longum* by amoxicillin allowed the gut microbiota of children with SAM to better adapt to a solid-food diet by reducing the abundance of taxa specialized for breast milk utilization, resulting in improved anthropometric indicators of infant nutritional status[97]. However, it is essential to note that *B. longum* subspecies *infantis* is a critical early infant gut bacteria with important benefits for infant health, including protection from enteric pathogens[98], immune system development[99], and reducing asthma risk[100]. *B. longum* subspecies *infantis* also improved ponderal growth when administered to infants ~4mo of age with SAM in two RCTs[101,102]. However, the effects on LAZ were not statistically significant. Our work complements this literature. Our findings suggest that a shift to away from a “less mature” microbiome, characterized by a high abundance of *B. longum* and carriage of strains that are better suited to HMO metabolism, may be critical to support efficacy of nutrient supplements that start with the introduction of complementary feeding; and we identify maternal drivers of early infant *B. longum* abundance and strain carriage which, if further elucidated, may be employed to shape the infant microbiome into a more favorable composition at this critical time in infancy.

There are some limitations of this work. First, from our cohort of 1169 HIV-unexposed, uninfected infants, we had microbiome data on 172 infants. However, infants included in our analyses were comparable to excluded infants (Table S6). Also, mother-infant FUT2+/FUT3- phenotype, which was an important determinant of *B. longum* abundance and strain cluster detection, did modify the impact of IYCF on infant growth in the larger sample of 792 infants without measured microbiome data in a way that was consistent with our microbiome results. That said, our small sample size may have limited power to detect effect modification by other taxa that are indicative of a "more mature" post-weaning microbiome. Finally, our analyses were not able to investigate effect modification by actual microbial metabolic activity, maternal HMO composition or infant gut glycobiome, which would require multi-omics approaches such as metatranscriptomics and metabolomics.

In conclusion, we present analyses of moderators of IYCF impact on infant stunting at 18mo in an RCT of IYCF using SQ-LNS in rural Zimbabwe. We report that (i) the impact of IYCF on stunting risk at 18mo is reduced by infant age-related changes in microbiome species composition characterized by a shift from *B. longum* dominance, particularly *B. longum* strains that are most similar to the proficient HMO utilizer subspecies *infantis;* (ii) discordance in mother-infant FUT2+/FUT3- phenotype was associated with reduced IYCF impact on stunting risk; and (iii) *B. longum* relative abundance was also determined by mother-infant FUT2+/FUT3- phenotype. Future work should investigate how differences between materanal HMOs and infant HBGAs determine gut Bifidobacterium species and strain composition, and investigate how to tailor interventions at the introduction of complementary feeding to balance infant nutritional needs with age-related microbiome composition and function to prevent stunting.

Figure legends

Figure 1. Infant growth trajectories and growth velocities vary by IYCF arm and mother-infant FUT2+/FUT3- phenotype.

(A) LAZ by infant age from 1-18mo (n=792), stratified by IYCF arm (light grey, no IYCF; dark grey, IYCF) and mother-infant FUT2+/FUT3- phenotype (*both*, *none*, *infant only* or *mother only*). Lines illustrate average trajectories. Shaded areas are 95% confidence bands. Infants randomized to IYCF in the *mother only* group had a less steep decline in LAZ trajectories on average compared to infants randomized to no IYCF.

(B) Violin plots of LAZ velocity from 6-18mo of age, stratified by IYCF arm (light grey, no IYCF; dark grey, IYCF) and mother-infant FUT2+/FUT3- phenotype (*both*, *none*, *infant only* or *mother only*). Open circles with error bars in the center of each panel indicate mean LAZ velocity and 95%CIs. All groups of infants had negative LAZ velocities on average, but infants in the *mother only* group who were randomized to IYCF had higher LAZ velocity on average, contributing to a less steep decline in LAZ over time and a smaller proportion of infants stunted at 18mo.

Figure 2. Infant growth trajectories and growth velocities vary by IYCF arm and infant gut *Bifidobacterium longum* relative abundance.

(A) LAZ by infant age from 1-18mo (n=53), stratified by IYCF arm and *Bifidobacterium longum* relative abundance (light grey, $\leq$median relative abundance; dark grey, >median relative abundance). Thin lines illustrate individual trajectories. Thick lines show average trajectories. Infants randomized to IYCF who were above the median relative abundance had a declining growth trajectory on average, while infants below the median did not.

(B) Violin plots of LAZ velocity from 6-18mo of age, stratified by IYCF arm (light grey, no IYCF; dark grey, IYCF) and mother-infant FUT2+/FUT3- phenotype (*both*, *none*, *infant only* or *mother only*). Open circles

521 with error bars indicate mean LAZ velocity and 95%CIs. All groups of infants had negative LAZ velocities
522 on average. However, LAZ velocity trended toward being higher in the group with relative abundance
523 below the median. The 95% confidence intervals overlap, but the higher LAZ velocity contributed to a
524 less steep decline in LAZ over time and a smaller proportion of stunted infants at 18mo.
525
526 **Figure 3. *Bifidobacterium longum* strains most similar to subspecies *infantis* dominate the early infant**
527 **gut microbiome.** Ordination plots of PCoA with Jaccard dissimilarities calculated using the pangenome
528 profiles of dominant *Bifidobacterium longum* strains in fecal specimens (N=284) generated using
529 PanPhlan3.0. Three clusters of *B. longum* strains were identifiable. Individual strains and indicated by
530 small circles. Those in the same cluster are enclosed by a large ellipse and are differentiated by both the
531 color of the ellipse and the border color of the small circle (blue, *infantis*; dark green, *longum*; red, *suis*).
532 Filled small circles indicate reference strains (light blue, *infantis*; pink, *suis*, light green, *longum*; grey,
533 *unclassified*). Open small circles indicate SHINE strains. Subspecies *infantis* reference strains
534 predominantly grouped with the largest cluster (blue ellipse, *infantis* cluster). Subspecies *longum*
535 reference strains predominantly grouped with the second largest cluster (dark green ellipse, *longum*
536 cluster). The remaining cluster (red ellipse, *suis* cluster) grouped with subspecies *suis* and *longum*.
537
538 **Figure 4. SHINE infant *Bifidobacterium longum infantis* cluster strains are better adapted for human**
539 **milk oligosaccharide utilization and protection against pathogens than *suis* and *longum* cluster strains.**
540 (A) Heatmap of UniProt gene family presence in SHINE infant *Bifidobacterium longum* strains (N=284).
541 UniProt gene family presence is indicated in grey. The horizontal bar at the top indicates strain cluster
542 (blue, *infantis*; dark green, *longum*; red, *suis*). Vertical bars from left to right indicate: UniProt gene
543 families that differed in prevalence between the *infantis* and *longum* cluster by two-sided Fisher's Exact
544 test after FDR correction (red); UniProt gene families that differed in prevalence between the *infantis*

and *suis* cluster by two-sided Fisher's Exact test after FDR correction (red); Biological Process GO groups; CAZymes; and Transporter class. Only gene families with evidence of overrepresentation in a Biological Process, CAZyme or Transporter class by one-sided Fisher's Exact Test are presented.

(B) Heatmap of MetaCyc pathway presence in SHINE infant *Bifidobacterium longum* strains (N=284). MetaCyc pathway presence is indicated in grey. The horizontal bar at the top indicates strain cluster (blue, *infantis*; dark green, *longum*; red, *suis*). Vertical bars from left to right indicate: MetaCyc pathways that differed in prevalence between the *infantis* and *longum* cluster by two-sided Fisher's Exact test after FDR correction (red); MetaCyc pathways that differed in prevalence between the *infantis* and *suis* cluster by two-sided Fisher's Exact test after FDR correction (red); MetaCyc pathway type. Only pathways with evidence of overrepresentation in a pathway type by one-sided Fisher's Exact Test are presented.

Figure S1. Flow chart of pathways for histo-blood group antigen synthesis by functional FUT2 and FUT3 status. The type 2 precursor includes β1-4 rather than β1-3 bonds and α1-3 rather than α1-4 bonds. The light-gray shaded region of the chart indicates non-secretor (FUT2-), Lewis-positive (FUT3+) pathways that produce the FUT2-/FUT3+ phenotype (Lewis Le^{a}). Pathways outside the light-gray shaded region of the chart produce secretor (FUT2+) phenotypes. In this outside region, the area enclosed by gray dashed lines indicates pathways that produce the FUT2+/FUT3+ (Lewis Le^{b}), while the area outside the gray dashed lines indicates the pathways that produce the FUT2+/FUT3- phenotype (Le^{a-b-}).

Figure S2. Flow of participants through the SHINE trial and the analyses reported in this study. The Sanitation Hygiene Infant Nutrition Efficacy (SHINE) trial enrolled 5280 pregnant women, of whom 3937 were HIV-negative. Of these HIV-negative pregnant women, 1153 and their 1169 live-born infants were recruited into a sub-study to investigate biomarkers of environmental enteric dysfunction. FUT2 and

FUT3 phenotypes were ascertained in 792 of these infants and their mothers. 172 of these infants provided at least 1 fecal specimen for shotgun metagenomic sequencing (354 fecal specimens). 218 of these fecal metagenomes, from 136 infants, plus an additional 66 fecal metagenomes from 43 infants in whom mother and infant FUT2 and FUT3 phenotypes were not ascertained, had sufficient coverage of the *Bifidobacterium longum* genome for pangenome analysis by PanPhlan3.0. 53 infants had metagenomic data at the 6mo follow-up visit and were included in regression analyses to determine effect modification of IYCF by the infant microbiome.

Figure S3. Infant age and mother-infant FUT2+/FUT3- phenotype significantly explain variation in infant gut microbiome composition. Ordination biplots for a multivariable constrained PCoA model that included both infant age and mother-infant FUT2+/FUT3- phenotype (N=354 metagenomes from 172 infants). The x-axis represents PCoA axis 1 scores in all panels.
(A) The y-axis represents PCoA axis 2, and points are colored from light pink to red to indicate younger to older infant age (mo) at which fecal specimens were taken.
(B-C) The y-axes represent PCoA axes 2-4, and points are colored to indicate mother-infant FUT2+/FUT3- phenotype concordance, (black, *both* mother and infant are FUT2+/FUT3-; red, *none* are FUT2+/FUT3-; green, *infant only* is a FUT2+/FUT3-; blue, *mother only* is a FUT2+/FUT3-). Arrows parallel to PCoA axes are correlated with PCoA scores and arrow length is proportional to the variance explained by a variable.

Figure S4. Infant age-related microbiome species turnover predominantly reflects decreased relative abundance of *Bifidobacterium longum* and increased abundance of *Prevotella copri*, *Faecalibacterium prausnitzii*, *Dorea longicatena*, and *Dorea formicigenerans*. Barplot of microbiome species (x-axis) versus the 20 highest and 20 lowest PCoA axis 1 loadings (y-axis) from a multivariable constrained PCoA model that included both infant age and mother-infant FUT2+/FUT3- phenotype (N=354 metagenomes

593 from 172 infants). Green bars indicate species positively loaded on PCoA axis 1 that are more abundant
594 with increasing infant age, and red bars indicate species negatively loaded on PCoA axis 1 that are less
595 abundant with increasing infant age.
596
597 **Figure S5. Mother-infant FUT2+/FUT3- phenotype-related microbiome species turnover**
598 **predominantly reflects increased relative abundance of *Bifidobacterium longum*.** Barplot of
599 microbiome species (x-axis) versus the 20 highest and 20 lowest PCoA axis 2 loadings (y-axis) from a
600 multivariable constrained PCoA model that included both infant age and mother-infant FUT2+/FUT3-
601 phenotype concordance (N=354 metagenomes from 172 infants). Green bars indicate species positively
602 loaded on PCoA axis 2 that, relative to the *both* group, are more abundant in infants in the *none*
603 FUT2+/FUT3- group and red bars indicate species negatively loaded on PCoA axis 2 that, relative to the
604 *both* group, are more abundant in infants in the *infant only* FUT2+/FUT3- group.
605
606 **Figure S6. Mother-infant FUT2+/FUT3- phenotype-related microbiome species turnover.** Barplot of
607 microbiome species (x-axis) versus the 20 highest and 20 lowest PCoA axis 3 loadings (y-axis) from
608 multivariable constrained PCoA model that included both infant age and mother-infant FUT2+/FUT3-
609 phenotype concordance (N=354 metagenomes from 172 infants). Green bars indicate species positively
610 loaded on PCoA axis 3 that, relative to the *both* group, are more abundant in infants the *mother only*
611 FUT2+/FUT3- group, and red bars indicate species negatively loaded on PCoA axis 3 that, relative to the
612 *both* group, are more abundant in infants in the *none* FUT2+/FUT3- group.
613
614 **Figure S7. Mother-infant FUT2+/FUT3- phentoype-related microbiome species turnover.** Barplot of
615 microbiome species (x-axis) versus the 20 highest and 20 lowest PCoA axis 4 loadings (y-axis) from a
616 multivariable constrained PCoA model that included both infant age and mother-infant FUT2+/FUT3-

phenotype concordance (N=354 metagenomes from 172 infants). Green bars indicate species positively loaded on PCoA axis 4 that, relative to the *both* group, are more abundant in infants in the *infant only* FUT2+/FUT3- group, and red bars indicate species negatively loaded on PCoA axis 4 that, relative to the *both* group, are more abundant in infants in the *mother only* FUT2+/FUT3- group.

Figure S8. *Bifidobacterium longum* strains most similar to subspecies *infantis* dominate the early infant gut microbiome. Heatmap of UniProt gene family presence in *B. longum* strains (N=284 SHINE strains and 118 reference strains). UniProt gene family presence is indicated in grey. The horizontal bars at the top from topmost to bottommost row indicate: strain source (black, reference strain; white, SHINE strain); reference strain subspecies (light blue, *infantis*; light green, *longum;* pink, *suis*; grey, *unclassified*), and strain cluster (blue, *infantis*; dark green, *longum*; red, *suis*). Clusters were defined by hierarchical clustering of Jaccard dissimilarities, and cluster membership was determined by cutting the cluster dendrogram at a height that would produce three clusters (horizontal gray line). Rows are ordered using the default hierarchical clustering settings of *heatmap3*.

Figure S9. SHINE infant *Bifidobacterium longum* strains in the *infantis* cluster differ from other infant *B. longum* strain clusters in their UniProt gene family profiles. Heatmap of UniProt gene family presence in SHINE infant *B. longum* strains (N=284). UniProt gene family presence is indicated in grey. The horizontal bar at the top indicates strain cluster (blue, *infantis*; dark green, *longum*; red, *suis*). Vertical bars from left to right indicate: UniProt gene families that differed in prevalence between the *infantis* and *longum* cluster by two-sided Fisher's Exact test after FDR correction (red); UniProt gene families that differed in prevalence between the *infantis* and *suis* cluster by two-sided Fisher's Exact test after FDR correction (red).

Figure S10. SHINE infant *Bifidobacterium longum* strains in the *infantis* cluster differ from other infant *B. longum* strain clusters in their MetaCyc pathway profiles. Heatmap of MetaCyc pathway presence in SHINE infant *B. longum* strains (N=284) as determined by MinPath. MetaCyc pathway presence is indicated in grey. The horizontal bar at the top indicates strain cluster (blue, *infantis*; dark green, *longum*; red, *suis*). Vertical bars from left to right indicate: MetaCyc pathways that differed in prevalence between the *infantis* and *longum* cluster by two-sided Fisher's Exact test after FDR correction (red); MetaCyc pathways that differed in prevalence between the *infantis* and *suis* cluster by two-sided Fisher's Exact test after FDR correction (red).

Figure S11. The infant gut microbiome undergoes a transition over time characterized by a decrease in *Bifidobacterium longum* relative abundance. Multivariable zero-inflated mixed-effects model fitted to longitudinal data (N=225 specimens from 87 infants). Infant age and mother-infant FUT2+/FUT3- phenotype were significant predictors of *B. longum* relative abundance. The model was used to predict the mean *B. longum* relative abundance (y-axis) which was plotted against infant age (mo) at follow-up (x-axis), conditional on model covariates. Mother-infant FUT2+/FUT3- phenotypes are differentiated by color (black, *both*; red, *none*; green, *infant only*; blue, *mother only* are FUT2+/FUT3-).

Figure S12. The infant gut microbiome undergoes a transition over time in which *Bifidobacterium longum* strains most similar to subspecies *infantis* become less prevalent and strains most similar to subspecies *suis* or *longum* become more prevalent. Multivariable logistic regression models were fitted to longitudinal data (N=133 specimens from 70 infants) with detection of each strain cluster as the dependent variable. A separate model was fitted for each strain cluster. Each model was used to predict the probability of detecting a *B. longum* strain in the specified cluster (y-axis) which was plotted against infant age (mo) at follow-up (x-axis), conditional on model covariates. Line colors indicate strain cluster

(blue, *infantis*; green, *longum*; red, *suis*). *Infantis* cluster strains were most likely to be detected throughout follow-up, but decreased in detection probability over time and was lowest at 18mo of age. While the probability of detecting *longum* and *suis* cluster strains increased with infant age. *Suis* cluster strain detection probabilities increased with age more than *longum* cluster strain detection and peaked at 18mo of age, where it was more likely to be detected than strains in the *infantis* cluster.

Figure S13. The dominance of *Bifidobacterium longum* strains most similar to subspecies *infantis* varies by mother-infant FUT2+/FUT3- phenotype. Multivariable logistic regression models were fitted to longitudinal data (N=133 specimens from 70 infants) with detection of each strain cluster as the dependent variable. A separate model was fitted for each strain cluster. Each model was used to predict the probability of detecting a *B. longum* strain in the specified cluster (y-axis) which was plotted against infant age (mo) at follow-up (x-axis) and mother-infant FUT2+/FUT3- phenotype, conditional on model covariates. Mother-infant FUT2+/FUT3- phenotypes are differentiated by color (black, *both*; red, *none*; green, *infant only*; blue, *mother only* are FUT2+/FUT3-). The *infant only* group had the highest probability of the *infantis* cluster throughout follow-up. While the *mother only* group had a lower probability of carrying an *infantis* cluster strain. The *mother only* group also had the highest probability of carrying a *suis* cluster strain.

(A) *infantis* cluster strain detection.

(B) *longum* cluster strain detection.

(C) *suis* cluster strain detection.

STAR Methods

Study design and participants

The Sanitation Hygiene Infant Nutrition Efficacy (SHINE) trial was a 2x2 factorial cluster-randomized trial that enrolled 5280 pregnant women at a median age of 12.5 weeks gestation between November 2012 and March 2015 to test the impact of improved household water quality, sanitation, and hygiene (WASH) and improved infant and young child feeding (IYCF) via provision of SQ-LNS to the infant from age 6mo-18mo, on linear growth and anemia at age 18mo. A detailed description of the SHINE trial design and methods has been published[51,103].

Briefly, research nurses made home visits twice during pregnancy and at infant ages 1, 3, 6, 12, and 18 months. At baseline, maternal education and age, household wealth[104], existing water and sanitation services, and household food security[105] were assessed, and mothers were tested for HIV via a rapid testing algorithm. Infant birth date, weight, and delivery details were transcribed from health facility records. Gestational age at delivery was calculated from the date of the mother's last menstrual period ascertained at baseline. Infant weight, length, and mid-upper arm circumference were measured at every postnatal visit. Nurses were standardized against a gold-standard anthropometrist every 6 months, with retraining provided to those who failed to meet predefined criteria.

Part-way through the trial (from mid-2014 onwards) mother-infant pairs were invited to join a substudy to collect additional biological specimens. Women were informed about the substudy at their 32-week gestation visit and those with live births were enrolled at the 1-month postnatal visit, or as soon as possible thereafter[106,107].

Specimen collection and processing

Mothers collected fecal specimens prior to the research nurse visit. Fecal specimens were placed in a cold box and transported to the field laboratory, where they were stored at -80°C until transfer to the central laboratory in Harare for long-term archiving at -80°C, with generator back-up. Fecal specimens were transferred via private courier on dry ice from Harare, Zimbabwe to Vancouver, British Columbia for metagenomic analyses.

The Qiagen DNeasy PowerSoil Kit was used to extract total DNA from 200mg of feces, according to manufacturer's instructions. Paired-end libraries were constructed using the Illumina TruSeq kit and using New England Biosystem TruSeq compatible library preparation reagents. Libraries were sequenced at the British Columbia Genome Sciences Centre using the Illumina HiSeq 2500 platform. Forty-eight libraries were pooled and included per sequencing lane. Negative controls were included to capture microbial contamination in the DNA extraction and library preparation steps.

The analyses presented here utilize data and specimens from HIV-uninfected mothers and their infants enrolled in the specimen collection substudy. The fecal microbiome was characterized in 354 specimens collected from 172 HIV-unexposed infants from 1 to 18mo of age. A mean(sd) of 2.0(1.0) samples were analyzed per child. Infants included in these analyses largely resembled the population of live-born infants from the wider SHINE trial who were not included in these analyses (Table S6). However, infants in the current analyses had slightly older mothers and longer gestational ages, and fewer were born during the hungry season, but more were in a household that met the minimum dietary diversity score (Table S6). Overall, the majority were born by vaginal delivery (91.6%) in an institution (91.5%) and were exclusively breastfed (83.2% at 3 months). The prevalence of stunting was 26.9% at 18mo in this sub-study (Table S6).

Bioinformatics

Sequenced reads were trimmed of adapters and filtered to remove low-quality, short (<60 base-pairs), and duplicate reads, as well as those of human, other animal or plant origin using KneadData with default settings. Overall, 354 unique whole metagenome sequencing datasets were used from fecal specimens collected from 1mo to 18mo from 172 infants with available mother and infant FUT2 and FUT3 phenotypes (Figure S2). On average, 10.8±3.7 million paired end quality-filtered reads were generated per sample. Assessment of negative controls and technical variation have been previously reported[64]. Species composition was determined by mapping reads to clade-specific markers using MetaPhlAn3, while functional gene and metabolic pathway composition was determined using HUMAnN3 against the UniRef90 database, both with default settings[52]. Bacterial species and pathway abundance estimates were normalized to relative abundances. UniProt gene family profiles were generated for dominant *B. longum* strains in fecal metagenomes with sufficient coverage for pangenome analysis using PanPhlan3[52]. To facilitate interpretation of UniProt gene family profiles, the minimum set of biological pathways sufficient to explain the gene families identified in each strain was determined using MinPath with default settings[58] and the MetaCyc database[57].

Assessment of FUT2 and FUT3 status

Saliva samples were collected by oral swab from mothers and infants. Available saliva from any follow-up visit was selected to assess FUT2 and FUT3 status. Secretor versus non-secretor (FUT2) and Lewis-positive versus Lewis-null (FUT3) status were ascertained for infants and their mothers using a previously reported phenotyping assay[108]. We defined FUT2 and FUT3 phenotype combinations as Lewis-positive non-secretors (FUT2-/FUT3+), Lewis-positive secretors (FUT+/FUT3+), or Lewis-null secretors (FUT2+/FUT3-) (Table S11) according to the histo-blood group antigen synthesis pathways

760 defined in Figure S1. Paired mother-infant phenotype concordance or discordance was defined as
761 presented in Table S1.
762 Of 1,169 mother-infant pairs, 999 (85.4%) mothers and 1104 (94.4%) infants were tested. Of these,
763 FUT2 or FUT3 status could be determined in 889 (76.0%) and 999 (85.4%) mothers and infants,
764 respectively (Table S11). Of those whose FUT2 or FUT3 status could be ascertained, secretors were the
765 most frequent FUT2 phenotype (88.1% and 85.6% in mothers and infants respectively), while Lewis-
766 positive was the most frequent FUT3 phenotype (76.8% and 74.9% in mothers and infants, respectively)
767 (Table S11). Most mothers and infants were Lewis-positive secretors (60.5% and 64.9%, respectively),
768 followed by FUT2+/FUT3- (25.1% and 23.2%, respectively), and Lewis-positive non-secretors (14.4% and
769 11.9%, respectively) (Table S1).
770
771 *Statistical analyses*

772 Infant characteristics that explain species β-diversity were evaluated using constrained principal
773 coordinates analysis (PCoA) of Bray-Curtis dissimilarities (*capscale*)[109]. Characteristics of interest
774 included factors that are known to be correlated with microbiome composition (infant age, sex, EBF at
775 3mo, dietary diversity, maternal and infant FUT2 and FUT3 phenotype). Statistical significance was
776 tested by permutational analysis of variance using distance matrices with 1000 permutations
777 (*adonis2*)[110]. We then developed a final multivariable constrained PCoA model that included covariates
778 which explained a significant fraction ($p<0.05$) of the variance in microbiome composition (infant age at
779 specimen collection), as well as mother-infant FUT2+/FUT3- discordance given our *a prior* hypothesis
780 that FUT2 and FUT3 phenotypes are important determinants of infant microbiome composition and our
781 finding that mother-infant FUT2+/FUT3- discordance was an important modifier of IYCF efficacy to
782 reduce stunting at 18mo. Constrained PCoA axis scores in the final multivariable model represented

783 changes in microbiome composition (species turnover) along gradients defined by each infant
784 characteristic included in the full model.

785 Since the IYCF intervention was started at the 6mo follow-up visit, we assessed interaction between
786 randomization to IYCF and mother-infant FUT2+/FUT3- discordance or microbiome composition using
787 data from the 6mo visit as covariates. The primary outcome was stunting at 18mo and LAZ at 18mo was
788 a secondary outcome. We fitted separate models for stunting and LAZ at 18mo. Interaction was
789 assessed on the additive risk difference scale, which is most appropriate for statistical estimation of
790 synergistic biological effects[111]. We used generalized linear models (*glm*) with a Gaussian distribution, an
791 identity link, sandwich standard errors (*sandwich*)[112] and an IYCF-by-mother-infant FUT2+/FUT3-
792 phenotype interaction term. We repeated these analyses using IYCF-by-PCoA axis score interaction
793 terms, where PCoA axis scores were derived from the final multivariable constrained PCoA model. One
794 model was fitted per constrained PCoA axis. For species that were strongly associated with PCoA axis
795 scores (loadings > 0.5 or < -0.5), analyses were repeated to assess IYCF-by-species interactions. We fitted
796 a separate model for each species of interest. Models also included IYCF, infant sex, mother-infant
797 FUT2+/FUT3- discordance, infant age at specimen collection, an indicator of whether infants met the
798 minimum dietary diversity score at specimen collection, and LAZ at specimen collection. We did not
799 include WASH arm because, in prior analyses, the SHINE WASH intervention did not affect stunting or
800 LAZ at 18mo[51] nor infant gut microbiome composition[64]. P-values were adjusted for multiple hypothesis
801 testing to preserve the false discovery rate[113].
802
803 *Identification and analysis of Bifidobacterium longum strain clusters*
804 *B. longum* strain profiles produced with PanPhlan3.0, which indicate whether UniProt gene families
805 are present in a strain[114], were converted to Jaccard dissimilarity matrices and visualized by PCoA to
806 ascertain the existence of strain clusters (*capscale*). Three clusters were identified, and strain cluster

807 membership was determined by hierarchical clustering of Jaccard dissimilarities and Ward's error sum of
808 squares algorithm (*hclust*)[115]. Hierarchical clustering dendrograms were cut at a height to obtain three
809 clusters.

810 Differences in UniProt gene family profiles between *B. longum* strain clusters were determined by
811 two-sided Fisher's Exact test (*fisher.test*), with adjustment for multiple hypothesis testing to preserve
812 the false discovery rate[113], and were visualized using heatmaps (*heatmap3*). 3260 UniProt gene families
813 were differentially present between strain clusters after FDR-adjustment. We performed
814 overrepresentation analyses[53] using one-sided Fisher's Exact tests (*fisher.test*) to determine whether the
815 differentially present gene families were more likely to function as particular CAZymes[55] or
816 transporters[56], or in specific GO biological processes[54]. These analyses were repeated using the
817 biological pathways determined with MinPath[58]. 115 pathways were differentially present between
818 strain clusters after FDR-adjustment. We performed overrepresentation analyses of these pathways to
819 determine whether they were more likely to have particular biological functions defined by MetaCyc
820 pathway types.

821

822 *Predictors of Bifidobacterium relative abundance and strain detection*

823 Predictors of *B. longum* relative abundance over time were assessed using mixed-effects zero-
824 inflated beta regression estimated by restricted maximum likelihood (*gamlss*)[116]. The model included
825 infant age at specimen collection, sex, EBF at 3mo, minimum infant dietary diversity at specimen
826 collection, and mother-infant FUT2+/FUT3- discordance, with random intercepts (*re*) and a first order
827 autocorrelation structure (*corCAR1*).

828 Predictors of *B. longum* strain cluster were assessed by logistic regression (*glm*) using an indicator of
829 strain cluster presence as the dependent variable, with the same covariates, and sandwich standard
830 errors. An individual model was fitted separately for each cluster. Bias corrected[117] logistic regression

was used to facilitate stable parameter estimation due to separation resulting from the small sample size[118].

All statistical analyses were conducted in R version 4.2.0. PCoA and adonis2 were performed using the *vegan* package[119]. Heatmaps were generated with *heatmap3*. Mixed-effects zero-inflated beta regression was performed using the *gamlss* package[120]. Bias corrected logistic regression models were fitted using the *brglm2* package. Sandwich standard errors were generated with the *sandwich* package.

Ethics approvals

All SHINE mothers provided written informed consent. The Medical Research Council of Zimbabwe (MRCZ/A/1675), Johns Hopkins Bloomberg School of Public Health (JHU IRB # 4205.), and the University of British Columbia Ethics Board (H15-03074) approved the study protocol, including the microbiome analyses. The SHINE trial is registered at ClinicalTrials.gov (NCT01824940).

Acknowledgments

We thank all the mothers, babies, and their families who participated in the SHINE trial and all members of the SHINE trial team (all members listed here: https://doi.org/10.1093/cid/civ844). We particularly thank the leadership and staff of the Ministry of Health and Child Care in Chirumanzu and Shurugwi districts and Midlands Province (especially environmental health, nursing, and nutrition) for their roles in operationalization of the study procedures, the Ministry of Local Government officials in each district who supported and facilitated field operations, Phillipa Rambanepasi and her team for proficient management of all the finances, Virginia Sauramba for management of compliance issues, and the programme officers at the Bill & Melinda Gates Foundation and the Department for International Development (UK Aid), who enthusiastically worked with us over a long period to make SHINE happen.

854 Funding was from the Bill & Melinda Gates Foundation (OPP1021542 and OPP1143707; J.H.H. and
855 A.J.P.), with a subcontract to the University of British Columbia (20R25498; A.R.M.). United Kingdom
856 Department for International Development (DFID/UKAID; J.H.H. and A.J.P.). Wellcome Trust
857 (093768/Z/10/Z, 108065/Z/15/Z, 206455/Z/17/Z, 203905/Z/16/Z and 210807/Z/18/Z; A.J.P., R.C.R. and
858 C.E.). Swiss Agency for Development and Cooperation (J.H.H. and A.J.P.). US National Institutes of Health
859 (2R01HD060338-06; J.H.H.). UNICEF (PCA-2017-0002; J.H.H. and A.J.P.). The Nutricia Research
860 Foundation (2021-52; E.K.G.) The funders had no role in the design of the study and collection, analysis,
861 and interpretation of data and in writing the manuscript.

862

863 **Author contributions**: A.R.M., L.E.S., R.J.S., M.N.N.M., J.H.H. and A.J.P. conceptualized and designed the
864 study. K.M., R.N., B.C., F.D.M., N.V.T., J.T., and B.M. collected data and biospecimens. H.M.G., I.B.,
865 S.K.G., R.C.R., F.F. and L.C. processed fecal specimens. M.K. conducted laboratory analyses to ascertain
866 FUT2 and FUT3 status. C.E., J.C. and E.K.G. developed the FUT2 and FUT3 analysis plan. E.K.G. developed
867 and conducted the microbiome statistical analysis plan. T.J.E. and E.K.G. conducted bioinformatics.
868 A.R.M. and E.K.G. analyzed and interpreted the data. E.K.G. wrote the original manuscript draft. All
869 authors reviewed the manuscript. A.R.M., A.J.P. and J.H.H. supervised and verified the data.

870

871 **Declaration of interests**: T.J.E. was paid a scientific consulting fee in relation to the analysis of the data
872 presented here by the Zvitambo Institute for Maternal and Child Health Research. All other authors
873 declare no competing interests.

874

875

876

877 **References**

878 1. United Nations Children's Fund, World Health Organization, and The World Bank (2019). Levels
879 and trends in child malnutrition: key findings of the 2019 Edition of the Joint Child Malnutrition
880 Estimates – UNICEF Regions. (United Nations Children's Fund (UNICEF), World Health Organization,
881 International Bank for Reconstruction and Development/The World Bank).

882 2. Onis, M.D., Garza, C., Onyango, A.W., and Martorell, R. (2006). WHO child growth standards. Acta
883 Paediatrica *95*, 1–104.

884 3. Benjamin-Chung, J., Mertens, A., Colford, J.M., Hubbard, A.E., van der Laan, M.J., Coyle, J.,
885 Sofrygin, O., Cai, W., Nguyen, A., Pokpongkiat, N.N., et al. (2023). Early-childhood linear growth
886 faltering in low- and middle-income countries. Nature *621*, 550–557.

887 4. Gough, E.K., Moodie, E.E.M., Prendergast, A.J., Ntozini, R., Moulton, L.H., Humphrey, J.H., Manges,
888 A.R., Stephens, D.A., Moodie, E.E.M., Prendergast, A.J., et al. (2016). Linear growth trajectories in
889 Zimbabwean infants. American Journal of Clinical Nutrition *104*, 1616–1627.

890 5. Adair, L.S.L.L.S., Fall, C.H.D.D., Osmond, C., Stein, A.D.A.A.D., Martorell, R., Ramirez-Zea, M.,
891 Sachdev, H.S., Dahly, D.L., Bas, I., Norris, S.A., et al. (2013). Associations of linear growth and
892 relative weight gain during early life with adult health and human capital in countries of low and
893 middle income: Findings from five birth cohort studies. The Lancet *382*, 525–534.

894 6. Victora, C.G., Adair, L., Fall, C., Hallal, P.C., Martorell, R., Richter, L., and Sachdev, H.S. (2008).
895 Maternal and child undernutrition: consequences for adult health and human capital. Lancet *371*,
896 340–357.

897 7. Vollmer, S., Harttgen, K., Subramanyam, M.A., Finlay, J., Klasen, S., and Subramanian, S.V. (2014).
898 Association between economic growth and early childhood undernutrition: evidence from 121
899 Demographic and Health Surveys from 36 low-income and middle-income countries. The Lancet
900 Global Health *2*, e225-234.

901 8. Dewey, K.G., Wessells, K.R., Arnold, C.D., Prado, E.L., Abbeddou, S., Adu-Afarwuah, S., Ali, H.,
902 Arnold, B.F., Ashorn, P., Ashorn, U., et al. (2021). Characteristics that modify the effect of small-
903 quantity lipid-based nutrient supplementation on child growth: an individual participant data
904 meta-analysis of randomized controlled trials. Am J Clin Nutr *114*, 15S-42S.

905 9. Dewey, K.G., Arnold, C.D., Wessells, K.R., Prado, E.L., Abbeddou, S., Adu-Afarwuah, S., Ali, H.,
906 Arnold, B.F., Ashorn, P., Ashorn, U., et al. (2022). Preventive small-quantity lipid-based nutrient
907 supplements reduce severe wasting and severe stunting among young children: an individual
908 participant data meta-analysis of randomized controlled trials. Am J Clin Nutr *116*, 1314–1333.

909 10. Ruel, M.T., Alderman, H., and Maternal Child Nutrition Study Group (2013). Nutrition-sensitive
910 interventions and programmes: how can they help to accelerate progress in improving maternal
911 and child nutrition? Lancet *382*, 536–551.

912 11. Arrieta, M.-C., Stiemsma, L.T., Amenyogbe, N., Brown, E.M., and Finlay, B. (2014). The intestinal
913 microbiome in early life: health and disease. Frontiers in Immunology *5*, 427.

12. Jones, H.J., Bourke, C.D., Swann, J.R., and Robertson, R.C. (2023). Malnourished Microbes: Host–Microbiome Interactions in Child Undernutrition. Annual Review of Nutrition *43*, 327–353.

13. Robertson, R.C., Manges, A.R., Finlay, B.B., and Prendergast, A.J. (2019). The Human Microbiome and Child Growth - First 1000 Days and Beyond. Trends Microbiol *27*, 131–147.

14. Subramanian, S., Huq, S., Yatsunenko, T., Haque, R., Mahfuz, M., Alam, M.A., Benezra, A., DeStefano, J., Meier, M.F., Muegge, B.D., et al. (2014). Persistent gut microbiota immaturity in malnourished Bangladeshi children. Nature *510*, 417–421.

15. Zhao, G., Vatanen, T., Droit, L., Park, A., Kostic, A.D., Poon, T.W., Vlamakis, H., Siljander, H., Härkönen, T., Hämäläinen, A.M., et al. (2017). Intestinal virome changes precede autoimmunity in type I diabetes-susceptible children. Proceedings of the National Academy of Sciences of the United States of America *114*, E6166–E6175. 10.1073/pnas.1706359114.

16. Ho, N.T., Li, F., Lee-Sarwar, K.A., Tun, H.M., Brown, B.P., Pannaraj, P.S., Bender, J.M., Azad, M.B., Thompson, A.L., Weiss, S.T., et al. (2018). Meta-analysis of effects of exclusive breastfeeding on infant gut microbiota across populations. Nature Communications *9*, 4169. 10.1038/s41467-018-06473-x.

17. Reyes, A., Blanton, L.V., Cao, S., Zhao, G., Manary, M., Trehan, I., Smith, M.I., Wang, D., Virgin, H.W., Rohwer, F., et al. (2015). Gut DNA viromes of Malawian twins discordant for severe acute malnutrition. Proceedings of the National Academy of Sciences of the United States of America *112*, 11941–11946. 10.1073/pnas.1514285112.

18. Gough, E.K., Stephens, D.A., Moodie, E.M., Prendergast, A.J., Stoltzfus, R.J., Humphrey, J.H., and Manges, A.R. (2016). Linear growth faltering in infants is associated with Acidaminococcus sp. and community-level changes in the gut microbiota. Microbiome *3*, 24.

19. Ghosh, T.S., Gupta, S.S., Bhattacharya, T., Yadav, D., Barik, A., Chowdhury, A., Das, B., Mande, S.S., and Nair, G.B. (2014). Gut Microbiomes of Indian Children of Varying Nutritional Status. PLoS ONE *9*, e95547.

20. Gupta, S.S., Mohammed, M.H., Ghosh, T.S., Kanungo, S., Nair, G.B., and Mande, S.S. (2011). Metagenome of the gut of a malnourished child. Gut Pathog *3*, 7.

21. Huey, S.L., Jiang, L., Fedarko, M.W., McDonald, D., Martino, C., Ali, F., Russell, D.G., Udipi, S.A., Thorat, A., Thakker, V., et al. (2020). Nutrition and the Gut Microbiota in 10- to 18-Month-Old Children Living in Urban Slums of Mumbai, India. mSphere *5*, e00731-20.

22. Digitale, J., Sié, A., Coulibaly, B., Ouermi, L., Dah, C., Tapsoba, C., Bärnighausen, T., Lebas, E., Arzika, A.M., Glymour, M.M., et al. (2020). Gut Bacterial Diversity and Growth among Preschool Children in Burkina Faso. Am J Trop Med Hyg *103*, 2568–2573.

23. Collard, J.-M., Andrianonimiadana, L., Habib, A., Rakotondrainipiana, M., Andriantsalama, P., Randriamparany, R., Rabenandrasana, M. a. N., Weill, F.-X., Sauvonnet, N., Randremanana, R.V., et al. (2022). High prevalence of small intestine bacteria overgrowth and asymptomatic carriage of enteric pathogens in stunted children in Antananarivo, Madagascar. PLoS Negl Trop Dis *16*, e0009849.

24. Kamng'ona, A.W., Young, R., Arnold, C.D., Kortekangas, E., Patson, N., Jorgensen, J.M., Prado, E.L., Chaima, D., Malamba, C., Ashorn, U., et al. (2019). The association of gut microbiota characteristics in Malawian infants with growth and inflammation. Scientific Reports *9*.

25. Perin, J., Burrowes, V., Almeida, M., Ahmed, S., Haque, R., Parvin, T., Biswas, S., Azmi, I.J., Bhuyian, S.I., Talukder, K.A., et al. (2020). A Retrospective Case-Control Study of the Relationship between the Gut Microbiota, Enteropathy, and Child Growth. The American journal of tropical medicine and hygiene.

26. Brown, E.M., Wlodarska, M., Willing, B. p, Vonaesch, P., Han, J., Reynolds, L.A., Arriet, M.-C., Uhrig, M., Scholz, R., Partida, O., et al. (2015). Diet and specific microbial exposure trigger features of environmental enteropathy in a novel murine model. Nature Communications *6*, 7806.

27. Kau, A.L., Planer, J.D., Liu, J., Rao, S., Yatsunenko, T., Trehan, I., Manary, M.J., Liu, T.-C., Stappenbeck, T.S., Maleta, K.M., et al. (2015). Functional characterization of IgA-targeted bacterial taxa from undernourished Malawian children that produce diet-dependent enteropathy. Science Translational Medicine *7*, 276ra24-276ra24.

28. Salli, K., Hirvonen, J., Siitonen, J., Ahonen, I., Anglenius, H., and Maukonen, J. (2021). Selective Utilization of the Human Milk Oligosaccharides 2□-Fucosyllactose, 3-Fucosyllactose, and Difucosyllactose by Various Probiotic and Pathogenic Bacteria. Journal of Agricultural and Food Chemistry *69*.

29. Davis, J.C.C., Totten, S.M., Huang, J.O., Nagshbandi, S., Kirmiz, N., Garrido, D.A., Lewis, Z.T., Wu, L.D., Smilowitz, J.T., German, J.B., et al. (2016). Identification of Oligosaccharides in Feces of Breast-fed Infants and Their Correlation with the Gut Microbial Community*. Molecular & Cellular Proteomics *15*, 2987–3002.

30. Charbonneau, M.R., O'Donnell, D., Blanton, L.V., Totten, S.M., Davis, J.C.C., Barratt, M.J., Cheng, J., Guruge, J., Talcott, M., Bain, J.R., et al. (2016). Sialylated Milk Oligosaccharides Promote Microbiota-Dependent Growth in Models of Infant Undernutrition. Cell *164*, 859–871.

31. Mank, M., Hauner, H., Heck, A.J.R., and Stahl, B. (2020). Targeted LC-ESI-MS2 characterization of human milk oligosaccharide diversity at 6 to 16 weeks post-partum reveals clear staging effects and distinctive milk groups. Anal Bioanal Chem *412*, 6887–6907.

32. Castanys-Muñoz, E., Martin, M.J., and Prieto, P.A. (2013). 2'-fucosyllactose: an abundant, genetically determined soluble glycan present in human milk. Nutr Rev *71*, 773–789.

33. Blank, D., Dotz, V., Geyer, R., and Kunz, C. (2012). Human milk oligosaccharides and Lewis blood group: individual high-throughput sample profiling to enhance conclusions from functional studies. Adv Nutr *3*, 440S-9S.

34. Schneider, M., Al-Shareffi, E., and Haltiwanger, R.S. (2017). Biological functions of fucose in mammals. Glycobiology *27*, 601–618.

35. Cooling, L. (2015). Blood groups in infection and host susceptibility. Clinical Microbiology Reviews *28*.

36. Tong, M., McHardy, I., Ruegger, P., Goudarzi, M., Kashyap, P.C., Haritunians, T., Li, X., Graeber, T.G., Schwager, E., Huttenhower, C., et al. (2014). Reprograming of gut microbiome energy metabolism by the FUT2 Crohn's disease risk polymorphism. ISME J *8*, 2193–2206.

37. Rausch, P., Rehman, A., Künzel, S., Häsler, R., Ott, S.J., Schreiber, S., Rosenstiel, P., Franke, A., and Baines, J.F. (2011). Colonic mucosa-associated microbiota is influenced by an interaction of crohn disease and FUT2 (Secretor) genotype. Proceedings of the National Academy of Sciences of the United States of America *108*.

38. Gampa, A., Engen, P.A., Shobar, R., and Mutlu, E.A. (2017). Relationships between gastrointestinal microbiota and blood group antigens. Physiol Genomics *49*, 473–483.

39. Wacklin, P., Mäkivuokko, H., Alakulppi, N., Nikkilä, J., Tenkanen, H., Räbinä, J., Partanen, J., Aranko, K., and Mättö, J. (2011). Secretor genotype (FUT2 gene) is strongly associated with the composition of bifidobacteria in the human intestine. PLoS ONE *6*, e20113.

40. Rühlemann, M.C., Hermes, B.M., Bang, C., Doms, S., Moitinho-Silva, L., Thingholm, L.B., Frost, F., Degenhardt, F., Wittig, M., Kässens, J., et al. (2021). Genome-wide association study in 8,956 German individuals identifies influence of ABO histo-blood groups on gut microbiome. Nat Genet *53*, 147–155.

41. Christensen, L., Vuholm, S., Roager, H.M., Nielsen, D.S., Krych, L., Kristensen, M., Astrup, A., and Hjorth, M.F. (2019). Prevotella Abundance Predicts Weight Loss Success in Healthy, Overweight Adults Consuming a Whole-Grain Diet Ad Libitum: A Post Hoc Analysis of a 6-Wk Randomized Controlled Trial. J Nutr *149*, 2174–2181.

42. Eriksen, A.K., Brunius, C., Mazidi, M., Hellström, P.M., Risérus, U., Iversen, K.N., Fristedt, R., Sun, L., Huang, Y., Nørskov, N.P., et al. (2020). Effects of whole-grain wheat, rye, and lignan supplementation on cardiometabolic risk factors in men with metabolic syndrome: a randomized crossover trial. Am J Clin Nutr *111*, 864–876. 10.1093/ajcn/nqaa026.

43. Shin, J.-H., Jung, S., Kim, S.-A., Kang, M.-S., Kim, M.-S., Joung, H., Hwang, G.-S., and Shin, D.-M. (2019). Differential Effects of Typical Korean Versus American-Style Diets on Gut Microbial Composition and Metabolic Profile in Healthy Overweight Koreans: A Randomized Crossover Trial. Nutrients *11*, E2450.

44. Hjorth, M.F., Roager, H.M., Larsen, T.M., Poulsen, S.K., Licht, T.R., Bahl, M.I., Zohar, Y., and Astrup, A. (2018). Pre-treatment microbial Prevotella-to-Bacteroides ratio, determines body fat loss success during a 6-month randomized controlled diet intervention. Int J Obes (Lond) *42*, 580–583.

45. Li, Y., Wang, D.D., Satija, A., Ivey, K.L., Li, J., Wilkinson, J.E., Li, R., Baden, M., Chan, A.T., Huttenhower, C., et al. (2021). Plant-Based Diet Index and Metabolic Risk in Men: Exploring the Role of the Gut Microbiome. J Nutr *151*, 2780–2789.

46. Li, J., Li, Y., Ivey, K.L., Wang, D.D., Wilkinson, J.E., Franke, A., Lee, K.H., Chan, A., Huttenhower, C., Hu, F.B., et al. (2022). Interplay between diet and gut microbiome, and circulating concentrations of trimethylamine N-oxide: findings from a longitudinal cohort of US men. Gut *71*, 724–733.

47. Wang, D.D., Nguyen, L.H., Li, Y., Yan, Y., Ma, W., Rinott, E., Ivey, K.L., Shai, I., Willett, W.C., Hu, F.B., et al. (2021). The gut microbiome modulates the protective association between a Mediterranean diet and cardiometabolic disease risk. Nat Med *27*, 333–343.

48. Hughes, R.L., Arnold, C.D., Young, R.R., Ashorn, P., Maleta, K., Fan, Y.-M., Ashorn, U., Chaima, D., Malamba-Banda, C., Kable, M.E., et al. (2020). Infant gut microbiota characteristics generally do not modify effects of lipid-based nutrient supplementation on growth or inflammation: secondary analysis of a randomized controlled trial in Malawi. Sci Rep *10*, 14861.

49. Smith, M.I., Yatsunenko, T., Manary, M.J., Trehan, I., Mkakosya, R., Cheng, J., Kau, A.L., Rich, S.S., Concannon, P., Mychaleckyj, J.C., et al. (2013). Gut microbiomes of Malawian twin pairs discordant for Kwashiorkor. Science *339*, 548–554.

50. Schwarzer, M., Makki, K., Storelli, G., Machuca-Gayet, I., Srutkova, D., Hermanova, P., Martino, M.E., Balmand, S., Hudcovic, T., Heddi, A., et al. (2016). Lactobacillus plantarum strain maintains growth of infant mice during chronic undernutrition. Science *351*, 854–857.

51. Humphrey, J.H., Mbuya, M.N.N., Ntozini, R., Moulton, L.H., Stoltzfus, R.J., Tavengwa, N.V., Mutasa, K., Majo, F.D., Mutasa, B., Mangwadu, G., et al. (2019). Independent and combined effects of improved water, sanitation, and hygiene, and improved complementary feeding, on child stunting and anaemia in rural Zimbabwe: a cluster-randomised trial. The Lancet Global Health *7*, e132–e147.

52. Beghini, F., McIver, L.J., Blanco-Míguez, A., Dubois, L., Asnicar, F., Maharjan, S., Mailyan, A., Manghi, P., Scholz, M., Thomas, A.M., et al. (2021). Integrating taxonomic, functional, and strain-level profiling of diverse microbial communities with bioBakery 3. Elife *10*, e65088.

53. Wieder, C., Frainay, C., Poupin, N., Rodríguez-Mier, P., Vinson, F., Cooke, J., Lai, R.P., Bundy, J.G., Jourdan, F., and Ebbels, T. (2021). Pathway analysis in metabolomics: Recommendations for the use of over-representation analysis. PLoS Comput Biol *17*, e1009105.

54. The Gene Ontology Consortium, Aleksander, S.A., Balhoff, J., Carbon, S., Cherry, J.M., Drabkin, H.J., Ebert, D., Feuermann, M., Gaudet, P., Harris, N.L., et al. (2023). The Gene Ontology knowledgebase in 2023. Genetics *224*, iyad031.

55. Drula, E., Garron, M.-L., Dogan, S., Lombard, V., Henrissat, B., and Terrapon, N. (2022). The carbohydrate-active enzyme database: functions and literature. Nucleic Acids Res *50*, D571–D577.

56. Saier, M.H., Reddy, V.S., Moreno-Hagelsieb, G., Hendargo, K.J., Zhang, Y., Iddamsetty, V., Lam, K.J.K., Tian, N., Russum, S., Wang, J., et al. (2021). The Transporter Classification Database (TCDB): 2021 update. Nucleic Acids Res *49*, D461–D467.

57. Caspi, R., Billington, R., Fulcher, C.A., Keseler, I.M., Kothari, A., Krummenacker, M., Latendresse, M., Midford, P.E., Ong, Q., Ong, W.K., et al. (2018). The MetaCyc database of metabolic pathways and enzymes. Nucleic Acids Research *46*, D633–D639.

58. Ye, Y., and Doak, T.G. (2009). A parsimony approach to biological pathway reconstruction/inference for genomes and metagenomes. PLoS Comput Biol *5*, e1000465.

59. Bazanella, M., Maier, T.V., Clavel, T., Lagkouvardos, I., Lucio, M., Maldonado-Gòmez, M.X., Autran, C., Walter, J., Bode, L., Schmitt-Kopplin, P., et al. (2017). Randomized controlled trial on the impact of early-life intervention with bifidobacteria on the healthy infant fecal microbiota and metabolome. American Journal of Clinical Nutrition *106*, 1274–1286.

60. Davenport, E.R., Cusanovich, D.A., Michelini, K., Barreiro, L.B., Ober, C., and Gilad, Y. (2015). Genome-wide association studies of the human gut microbiota. PLoS ONE *10*. 10.1371/journal.pone.0140301.

61. Turpin, W., Bedrani, L., Espin-Garcia, O., Xu, W., Silverberg, M.S., Smith, M.I., Guttman, D.S., Griffiths, A., Moayyedi, P., Panaccione, R., et al. (2018). FUT2 genotype and secretory status are not associated with fecal microbial composition and inferred function in healthy subjects. Gut Microbes *9*.

62. Bell, A., and Juge, N. (2021). Mucosal glycan degradation of the host by the gut microbiota. Glycobiology *31*, 691–696.

63. Colston, J.M., Taniuchi, M., Ahmed, T., Ferdousi, T., Kabir, F., Mduma, E., Nshama, R., Iqbal, N.T., Haque, R., Ahmed, T., et al. (2022). Intestinal Colonization With Bifidobacterium longum Subspecies Is Associated With Length at Birth, Exclusive Breastfeeding, and Decreased Risk of Enteric Virus Infections, but Not With Histo-Blood Group Antigens, Oral Vaccine Response or Later Growth in Three Birth Cohorts. Front Pediatr *10*, 804798.

64. Robertson, R.C., Edens, T.J., Carr, L., Mutasa, K., Gough, E.K., Evans, C., Geum, H.M., Baharmand, I., Gill, S.K., Ntozini, R., et al. (2023). The gut microbiome and early-life growth in a population with high prevalence of stunting. Nat Commun *14*, 654.

65. Stewart, C.J., Ajami, N.J., O'Brien, J.L., Hutchinson, D.S., Smith, D.P., Wong, M.C., Ross, M.C., Lloyd, R.E., Doddapaneni, H.V., Metcalf, G.A., et al. (2018). Temporal development of the gut microbiome in early childhood from the TEDDY study. Nature *562*, 583–588.

66. Yatsunenko, T., Rey, F.E., Manary, M.J., Trehan, I., Dominguez-Bello, M.G., Contreras, M., Magris, M., Hidalgo, G., Baldassano, R.N., Anokhin, A.P., et al. (2012). Human gut microbiome viewed across age and geography. Nature *486*, 222–228.

67. Marcobal, A., and Sonnenburg, J.L. (2012). Human milk oligosaccharide consumption by intestinal microbiota: Human milk oligosaccharide consumption. Clinical Microbiology and Infection *18*, 12–15.

68. Bäckhed, F., Roswall, J., Peng, Y., Feng, Q., Jia, H., Kovatcheva-Datchary, P., Li, Y., Xia, Y., Xie, H., Zhong, H., et al. (2015). Dynamics and stabilization of the human gut microbiome during the first year of life. Cell Host and Microbe *17*, 690–703. 10.1016/j.chom.2015.04.004.

69. Collado, M.C., Cernada, M., Baüerl, C., Vento, M., and Pérez-Martínez, G. (2012). Microbial ecology and host-microbiota interactions during early life stages. Gut Microbes *3*, 352–365.

70. Matamoros, S., Gras-Leguen, C., Vacon, F.L., Potel, G., and Cochetiere, M.-F. de L. (2013). Development of intestinal microbiota in infants and its impact on health. Trends in Microbiology *21*, 167–173.

71. Laursen, M.F. (2021). Gut Microbiota Development: Influence of Diet from Infancy to Toddlerhood. Annals of Nutrition and Metabolism.

72. Lewis, Z.T., Totten, S.M., Smilowitz, J.T., Popovic, M., Parker, E., Lemay, D.G., Van Tassell, M.L., Miller, M.J., Jin, Y.-S., German, J.B., et al. (2015). Maternal fucosyltransferase 2 status affects the gut bifidobacterial communities of breastfed infants. Microbiome *3*, 13.

73. Ojima, M.N., Jiang, L., Arzamasov, A.A., Yoshida, K., Odamaki, T., Xiao, J., Nakajima, A., Kitaoka, M., Hirose, J., Urashima, T., et al. (2022). Priority effects shape the structure of infant-type Bifidobacterium communities on human milk oligosaccharides. ISME J *16*, 2265–2279.

74. Li, M., Zhou, X., Stanton, C., Ross, R.P., Zhao, J., Zhang, H., Yang, B., and Chen, W. (2021). Comparative Genomics Analyses Reveal the Differences between B. longum subsp. infantis and B. longum subsp. longum in Carbohydrate Utilisation, CRISPR-Cas Systems and Bacteriocin Operons. Microorganisms *9*, 1713.

75. Gotoh, A., Katoh, T., Sakanaka, M., Ling, Y., Yamada, C., Asakuma, S., Urashima, T., Tomabechi, Y., Katayama-Ikegami, A., Kurihara, S., et al. (2018). Sharing of human milk oligosaccharides degradants within bifidobacterial communities in faecal cultures supplemented with Bifidobacterium bifidum. Scientific Reports *8*, 13958.

76. Sakanaka, M., Gotoh, A., Yoshida, K., Odamaki, T., Koguchi, H., Xiao, J.-Z., Kitaoka, M., and Katayama, T. (2019). Varied Pathways of Infant Gut-Associated Bifidobacterium to Assimilate Human Milk Oligosaccharides: Prevalence of the Gene Set and Its Correlation with Bifidobacteria-Rich Microbiota Formation. Nutrients *12*, 71. 10.3390/nu12010071.

77. Garrido, D., Ruiz-Moyano, S., Lemay, D.G., Sela, D.A., German, J.B., and Mills, D.A. (2015). Comparative transcriptomics reveals key differences in the response to milk oligosaccharides of infant gut-associated bifidobacteria. Sci Rep *5*, 13517.

78. Garrido, D., Ruiz-Moyano, S., Kirmiz, N., Davis, J.C., Totten, S.M., Lemay, D.G., Ugalde, J.A., German, J.B., Lebrilla, C.B., and Mills, D.A. (2016). A novel gene cluster allows preferential utilization of fucosylated milk oligosaccharides in Bifidobacterium longum subsp. longum SC596. Sci Rep *6*, 35045.

79. Vatanen, T., Ang, Q.Y., Siegwald, L., Sarker, S.A., Le Roy, C.I., Duboux, S., Delannoy-Bruno, O., Ngom-Bru, C., Boulangé, C.L., Stražar, M., et al. (2022). A distinct clade of Bifidobacterium longum in the gut of Bangladeshi children thrives during weaning. Cell *185*, 4280-4297.e12.

80. Sela, D.A., Chapman, J., Adeuya, A., Kim, J.H., Chen, F., Whitehead, T.R., Lapidus, A., Rokhsar, D.S., Lebrilla, C.B., German, J.B., et al. (2008). The genome sequence of Bifidobacterium longum subsp. infantis reveals adaptations for milk utilization within the infant microbiome. Proceedings of the National Academy of Sciences *105*, 18964–18969.

81. Thomson, P., Medina, D.A., and Garrido, D. (2018). Human milk oligosaccharides and infant gut bifidobacteria: Molecular strategies for their utilization. Food Microbiology *75*, 37–46.

82. LoCascio, R.G., Desai, P., Sela, D.A., Weimer, B., and Mills, D.A. (2010). Broad conservation of milk utilization genes in Bifidobacterium longum subsp. infantis as revealed by comparative genomic hybridization. Appl Environ Microbiol *76*, 7373–7381.

83. Fushinobu, S., and Abou Hachem, M. (2021). Structure and evolution of the bifidobacterial carbohydrate metabolism proteins and enzymes. Biochem Soc Trans *49*, 563–578.

84. Wei, X., Guo, Y., Shao, C., Sun, Z., Zhurina, D., Liu, D., Liu, W., Zou, D., Jiang, Z., Wang, X., et al. (2012). Fructose Uptake in Bifidobacterium longum NCC2705 Is Mediated by an ATP-binding Cassette Transporter. Journal of Biological Chemistry *287*, 357–367. 10.1074/jbc.M111.266213.

85. Johnstone, T.C., and Nolan, E.M. (2015). Beyond Iron: Non-Classical Biological Functions of Bacterial Siderophores. Dalton Trans *44*, 6320–6339.

86. Vazquez-Gutierrez, P., Lacroix, C., Jaeggi, T., Zeder, C., Zimmerman, M.B., and Chassard, C. (2015). Bifidobacteria strains isolated from stools of iron deficient infants can efficiently sequester iron. BMC Microbiol *15*, 3.

87. Vazquez-Gutierrez, P., de Wouters, T., Werder, J., Chassard, C., and Lacroix, C. (2016). High Iron-Sequestrating Bifidobacteria Inhibit Enteropathogen Growth and Adhesion to Intestinal Epithelial Cells In vitro. Front Microbiol *7*, 1480.

88. Gibson, G. r., and Wang, X. (1994). Regulatory effects of bifidobacteria on the growth of other colonic bacteria. Journal of Applied Bacteriology *77*, 412–420.

89. Arimond, M., Zeilani, M., Jungjohann, S., Brown, K.H., Ashorn, P., Allen, L.H., and Dewey, K.G. (2015). Considerations in developing lipid-based nutrient supplements for prevention of undernutrition: experience from the International Lipid-Based Nutrient Supplements (iLiNS) Project. Matern Child Nutr *11*, 31–61.

90. Beal, T., White, J.M., Arsenault, J.E., Okronipa, H., Hinnouho, G.-M., Murira, Z., Torlesse, H., and Garg, A. (2021). Micronutrient gaps during the complementary feeding period in South Asia: A Comprehensive Nutrient Gap Assessment. Nutr Rev *79*, 26–34.

91. White, J.M., Beal, T., Arsenault, J.E., Okronipa, H., Hinnouho, G.-M., Chimanya, K., Matji, J., and Garg, A. (2021). Micronutrient gaps during the complementary feeding period in 6 countries in Eastern and Southern Africa: a Comprehensive Nutrient Gap Assessment. Nutr Rev *79*, 16–25.

92. Park, J.J.H., Harari, O., Siden, E., Dron, L., Zannat, N.-E., Singer, J., Lester, R.T., Thorlund, K., and Mills, E.J. (2020). Interventions to improve linear growth during complementary feeding period for children aged 6-24 months living in low- and middle-income countries: a systematic review and network meta-analysis [version 2; peer review: 3 approved]. *3*, 1660.

93. Imdad, A., and Bhutta, Z.A. (2011). Effect of preventive zinc supplementation on linear growth in children under 5 years of age in developing countries: a meta-analysis of studies for input to the lives saved tool. BMC Public Health *11*, S22.

94. Ashorn, P., Alho, L., Ashorn, U., Cheung, Y.B., Dewey, K.G., Gondwe, A., Harjunmaa, U., Lartey, A., Phiri, N., Phiri, T.E., et al. (2015). Supplementation of Maternal Diets during Pregnancy and for 6

Months Postpartum and Infant Diets Thereafter with Small-Quantity Lipid-Based Nutrient Supplements Does Not Promote Child Growth by 18 Months of Age in Rural Malawi: A Randomized Controlled Trial. J Nutr *145*, 1345–1353. 10.3945/jn.114.207225.

95. Abellan-Schneyder, I., Matchado, M.S., Reitmeier, S., Sommer, A., Sewald, Z., Baumbach, J., List, M., and Neuhaus, K. (2021). Primer, Pipelines, Parameters: Issues in 16S rRNA Gene Sequencing. mSphere *6*, e01202-20.

96. Paganini, D., Uyoga, M.A., Kortman, G.A.M., Boekhorst, J., Schneeberger, S., Karanja, S., Hennet, T., and Zimmermann, M.B. (2019). Maternal Human Milk Oligosaccharide Profile Modulates the Impact of an Intervention with Iron and Galacto-Oligosaccharides in Kenyan Infants. Nutrients *11*, 2596.

97. Schwartz, D.J., Langdon, A., Sun, X., Langendorf, C., Berthé, F., Grais, R.F., Trehan, I., Isanaka, S., and Dantas, G. (2023). Effect of amoxicillin on the gut microbiome of children with severe acute malnutrition in Madarounfa, Niger: a retrospective metagenomic analysis of a placebo-controlled trial. The Lancet Microbe *4*, e931–e942.

98. Ruiz, L., Flórez, A.B., Sánchez, B., Moreno-Muñoz, J.A., Rodriguez-Palmero, M., Jiménez, J., Gavilán, C.G. de los R., Gueimonde, M., Ruas-Madiedo, P., and Margolles, A. (2020). Bifidobacterium longum subsp. infantis CECT7210 (B. infantis IM-1®) Displays In Vitro Activity against Some Intestinal Pathogens. Nutrients *12*, 3259.

99. Henrick, B.M., Rodriguez, L., Lakshmikanth, T., Pou, C., Henckel, E., Arzoomand, A., Olin, A., Wang, J., Mikes, J., Tan, Z., et al. (2021). Bifidobacteria-mediated immune system imprinting early in life. Cell *184*, 3884-3898.e11.

100. Dai, D.L.Y., Petersen, C., Hoskinson, C., Del Bel, K.L., Becker, A.B., Moraes, T.J., Mandhane, P.J., Finlay, B.B., Simons, E., Kozyrskyj, A.L., et al. (2023). Breastfeeding enrichment of B. longum subsp. infantis mitigates the effect of antibiotics on the microbiota and childhood asthma risk. Med *4*, 92-112.e5.

101. Barratt, M.J., Nuzhat, S., Ahsan, K., Frese, S.A., Arzamasov, A.A., Sarker, S.A., Islam, M.M., Palit, P., Islam, M.R., Hibberd, M.C., et al. (2022). Bifidobacterium infantis treatment promotes weight gain in Bangladeshi infants with severe acute malnutrition. Sci Transl Med *14*, eabk1107.

102. Nuzhat, S., Hasan, S.M.T., Palit, P., Islam, M.R., Mahfuz, M., Islam, M.M., Alam, M.A., Flannery, R.L., Kyle, D.J., Sarker, S.A., et al. (2023). Effects of probiotic and synbiotic supplementation on ponderal and linear growth in severely malnourished young infants in a randomized clinical trial. Sci Rep *13*, 1845.

103. Humphrey, J.H., Jones, A.D., Manges, A., Mangwadu, G., Maluccio, J.A., Mbuya, M.N.N., Moulton, L.H., Ntozini, R., Prendergast, A.J., Stoltzfus, R.J., et al. (2015). The sanitation hygiene infant nutrition efficacy (SHINE) Trial: Rationale, design, and methods. Clinical Infectious Diseases *61*, S685-702.

104. Chasekwa, B., Maluccio, J.A., Ntozini, R., Moulton, L.H., Wu, F., Smith, L.E., Matare, C.R., Stoltzfus, R.J., Mbuya, M.N.N., Tielsch, J.M., et al. (2018). Measuring wealth in rural communities: Lessons from the sanitation, hygiene, infant nutrition efficacy (SHINE) trial. PLoS ONE *13*, 1–19.

105. Maxwell, D., Watkins, B., Wheeler, R., and Collins, G. (2003). The Coping Strategy Index: a tool for rapid measurement of household food security and the impact of food aid programs in humanitarian emergencies. (CARE and WFP).

106. E.K, G., L.H, M., K, M., R, N., R.J, S., F.D, M., L.E, S., G, P., N, G., M, J., et al. (2020). Effects of improved water, sanitation, and hygiene and improved complementary feeding on environmental enteric dysfunction in children in rural Zimbabwe: A cluster-randomized controlled trial. PLoS Neglected Tropical Diseases *14*, e0007963.

107. Mutasa, K., Ntozini, R., Mbuya, M.N.N., Rukobo, S., Govha, M., Majo, F.D., Tavengwa, N., Smith, L.E., Caulfield, L., Swann, J.R., et al. (2021). Biomarkers of environmental enteric dysfunction are not consistently associated with linear growth velocity in rural Zimbabwean infants. The American journal of clinical nutrition *113*.

108. Colston, J.M., Francois, R., Pisanic, N., Yori, P.P., Mccormick, B.J.J., Olortegui, M.P., Gazi, M.A., Svensen, E., Ahmed, M.M.M., Mduma, E., et al. (2019). Effects of Child and Maternal Histo-Blood Group Antigen Status on Symptomatic and Asymptomatic Enteric Infections in Early Childhood. Journal of Infectious Diseases *220*, 151–162.

109. Legendre, P., and Anderson, M.J. (1999). Distance-Based Redundancy Analysis: Testing Multispecies Responses in Multifactorial Ecological Experiments. Ecological Monographs *69*, 1–24.

110. Anderson, M.J. (2001). A new method for non-parametric multivariate analysis of variance. Austral Ecology *26*, 32–46.

111. VanderWeele, T.J. (2012). Sample Size and Power Calculations for Additive Interactions. Epidemiol Methods *1*, 159–188.

112. Naimi, A.I., and Whitcomb, B.W. (2020). Estimating Risk Ratios and Risk Differences Using Regression. Am J Epidemiol *189*, 508–510.

113. Benjamini, Y., and Hochberg, Y. (1995). Controlling the False Discovery Rate: A Practical and Powerful Approach to Multiple Testing. Journal of the Royal Statistical Society. Series B (Methodological) *57*, 289–300.

114. Scholz, M., Ward, D.V., Pasolli, E., Tolio, T., Zolfo, M., Asnicar, F., Truong, D.T., Tett, A., Morrow, A.L., and Segata, N. (2016). Strain-level microbial epidemiology and population genomics from shotgun metagenomics. Nature Methods *13*, 435–438.

115. Murtagh, F., and Legendre, P. (2014). Ward's Hierarchical Agglomerative Clustering Method: Which Algorithms Implement Ward's Criterion? Journal of Classification *31*, 274–295.

116. Chen, E.Z., and Li, H. (2016). A two-part mixed-effects model for analyzing longitudinal microbiome compositional data. In Bioinformatics, pp. 2611–2617. 10.1093/bioinformatics/btw308.

117. Kosmidis, I., Kenne Pagui, E.C., and Sartori, N. (2020). Mean and median bias reduction in generalized linear models. Stat Comput *30*, 43–59.

118. Mansournia, M.A., Geroldinger, A., Greenland, S., and Heinze, G. (2018). Separation in Logistic Regression: Causes, Consequences, and Control. Am J Epidemiol *187*, 864–870.

119. Dixon, P. (2003). VEGAN, a package of R functions for community ecology. Journal of Vegetation Science *14*, 927–930.

120. Stasinopoulos, D.M., and Rigby, R.A. (2007). Generalized additive models for location scale and shape (GAMLSS) in R. Journal of Statistical Software *23*, 1–46. 10.18637/jss.v023.i07.

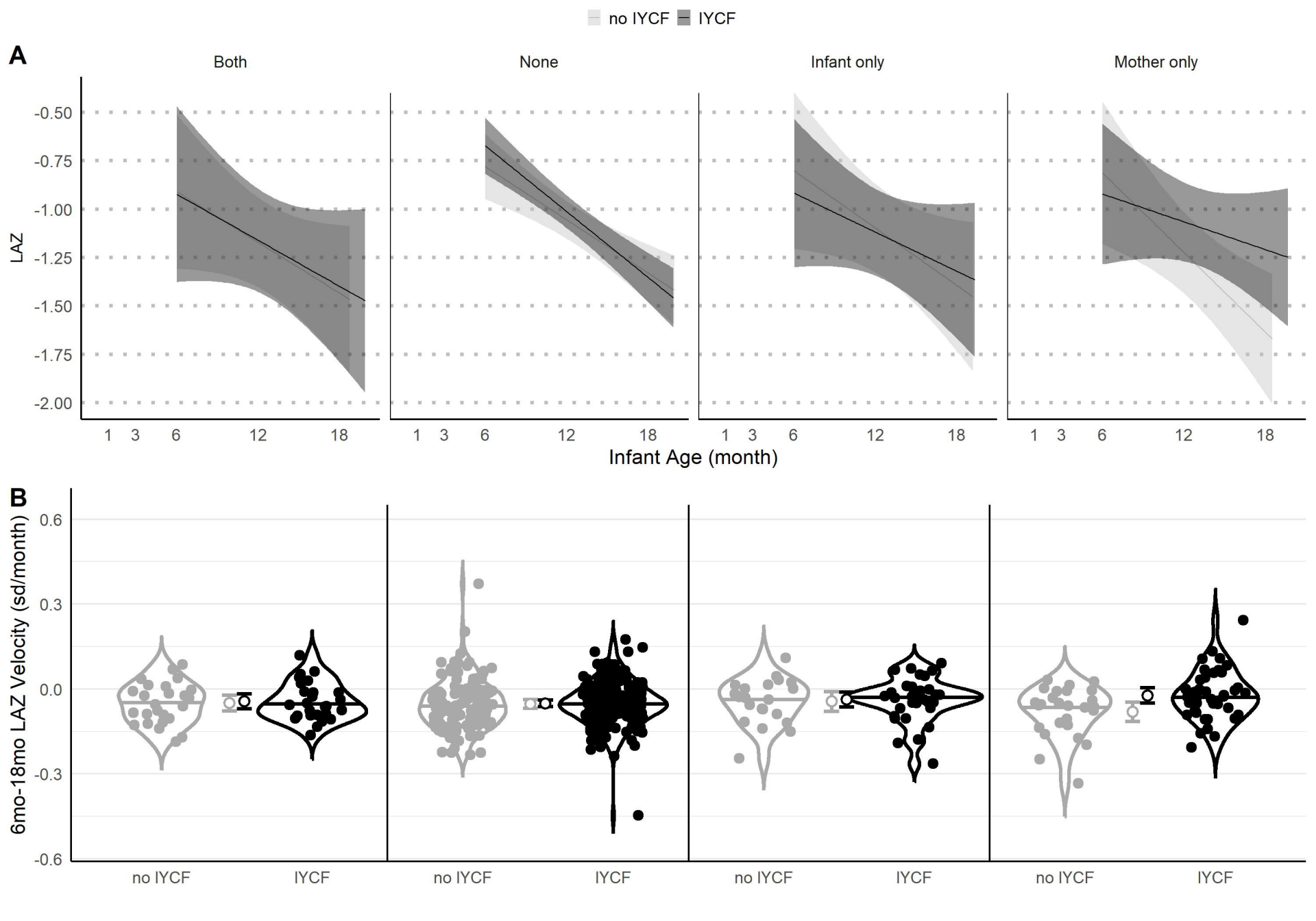
no IYCF
IYCF
A
Both
None
Infant only
Mother only
LAZ
-0.50
-0.75
-1.00
-1.25
-1.50
-1.75
-2.00
1
3
6
12
18
Infant Age (month)
B
6mo-18mo LAZ Velocity (sd/month)
0.6
0.3
0.0
-0.3
-0.6
no IYCF
IYCF

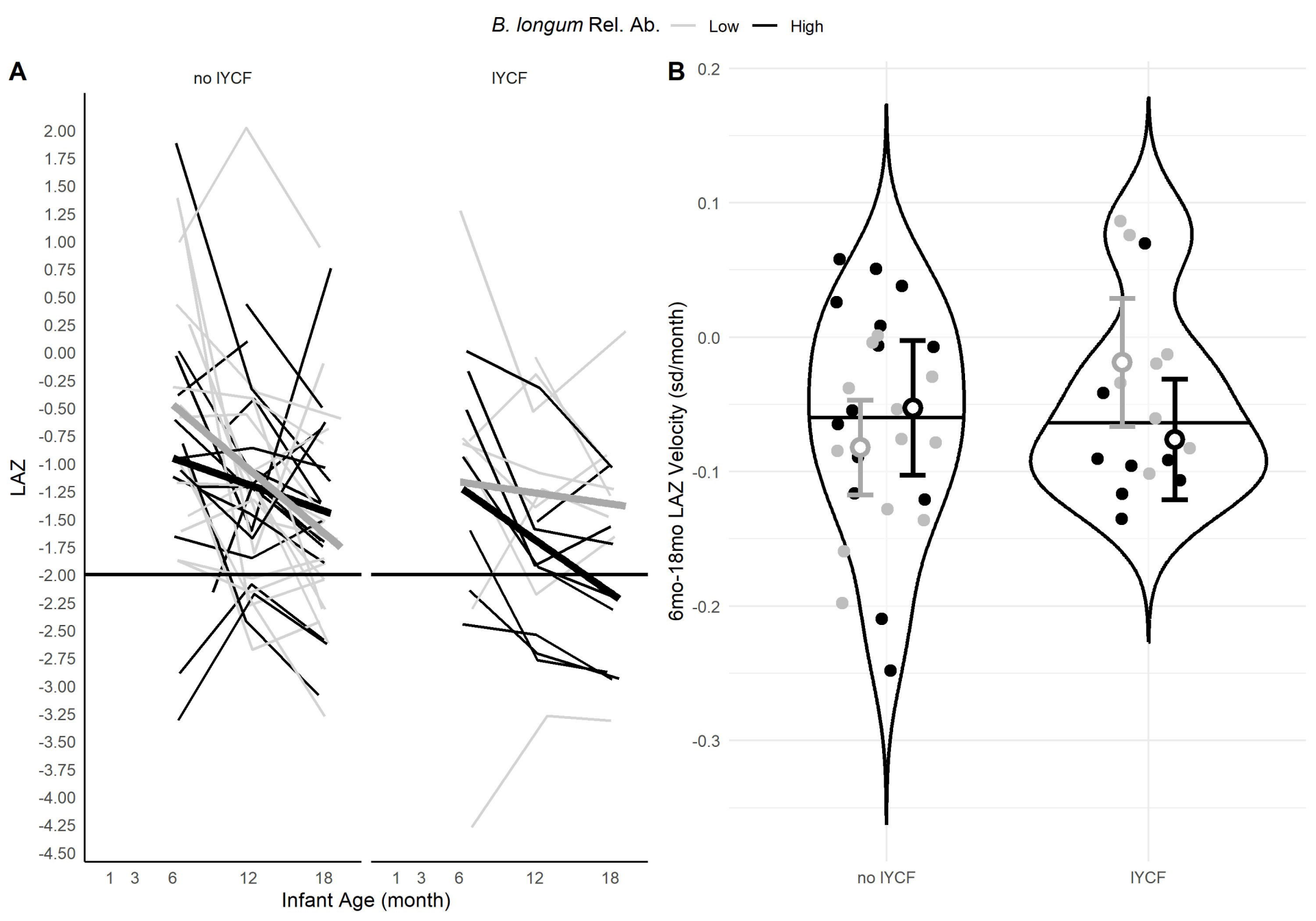
B. longum Rel. Ab.
Low
High
A
no IYCF
IYCF
LAZ
2.00
1.75
1.50
1.25
1.00
0.75
0.50
0.25
0.00
-0.25
-0.50
-0.75
-1.00
-1.25
-1.50
-1.75
-2.00
-2.25
-2.50
-2.75
-3.00
-3.25
-3.50
-3.75
-4.00
-4.25
-4.50
1
3
6
12
18
Infant Age (month)
B
6mo-18mo LAZ Velocity (sd/month)
0.2
0.1
0.0
-0.1
-0.2
-0.3
no IYCF
IYCF

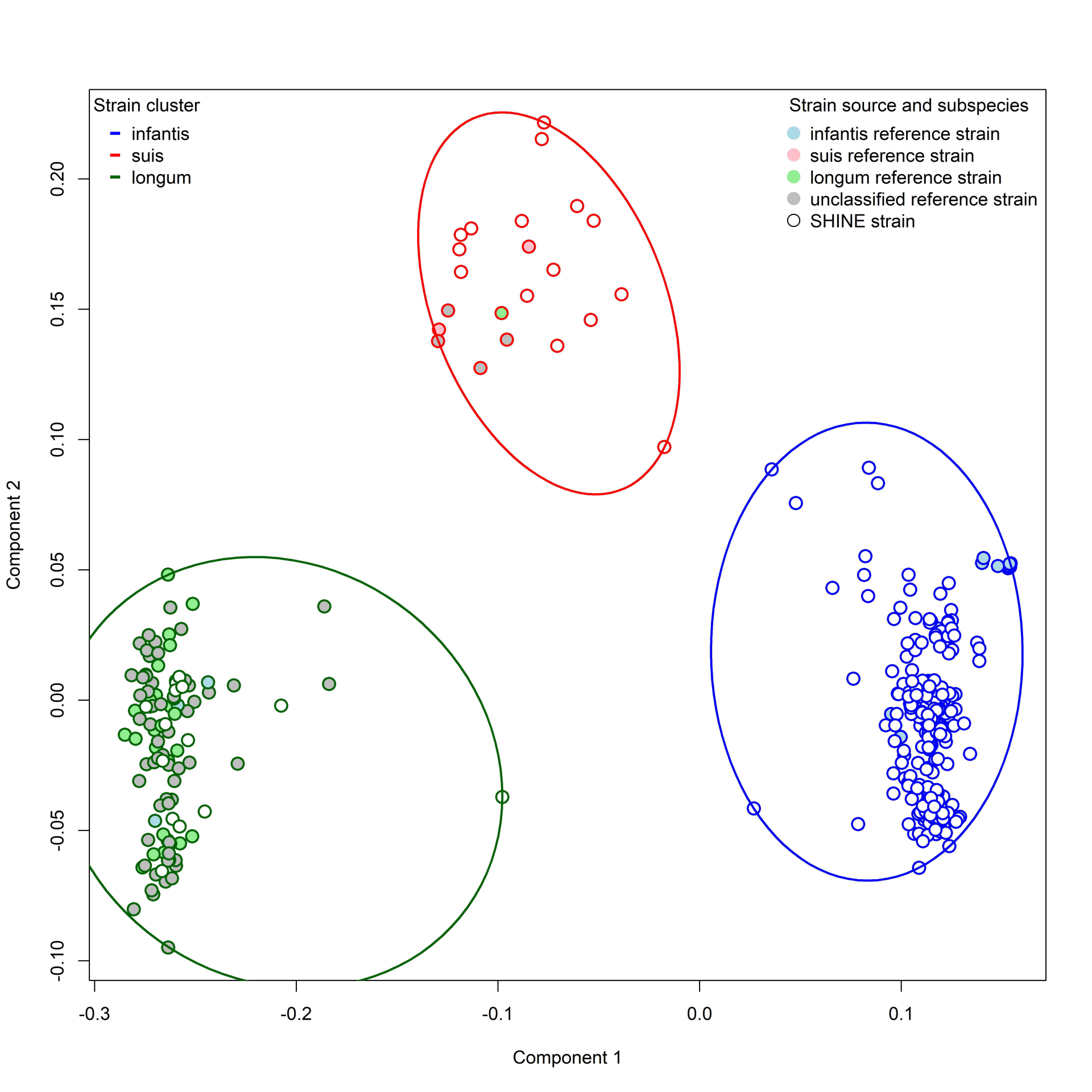
Strain cluster
infantis
suis
longum
Strain source and subspecies
infantis reference strain
suis reference strain
longum reference strain
unclassified reference strain
SHINE strain
Component 2
0.20
0.15
0.10
0.05
0.00
-0.05
-0.10
-0.3
-0.2
-0.1
0.0
0.1
Component 1

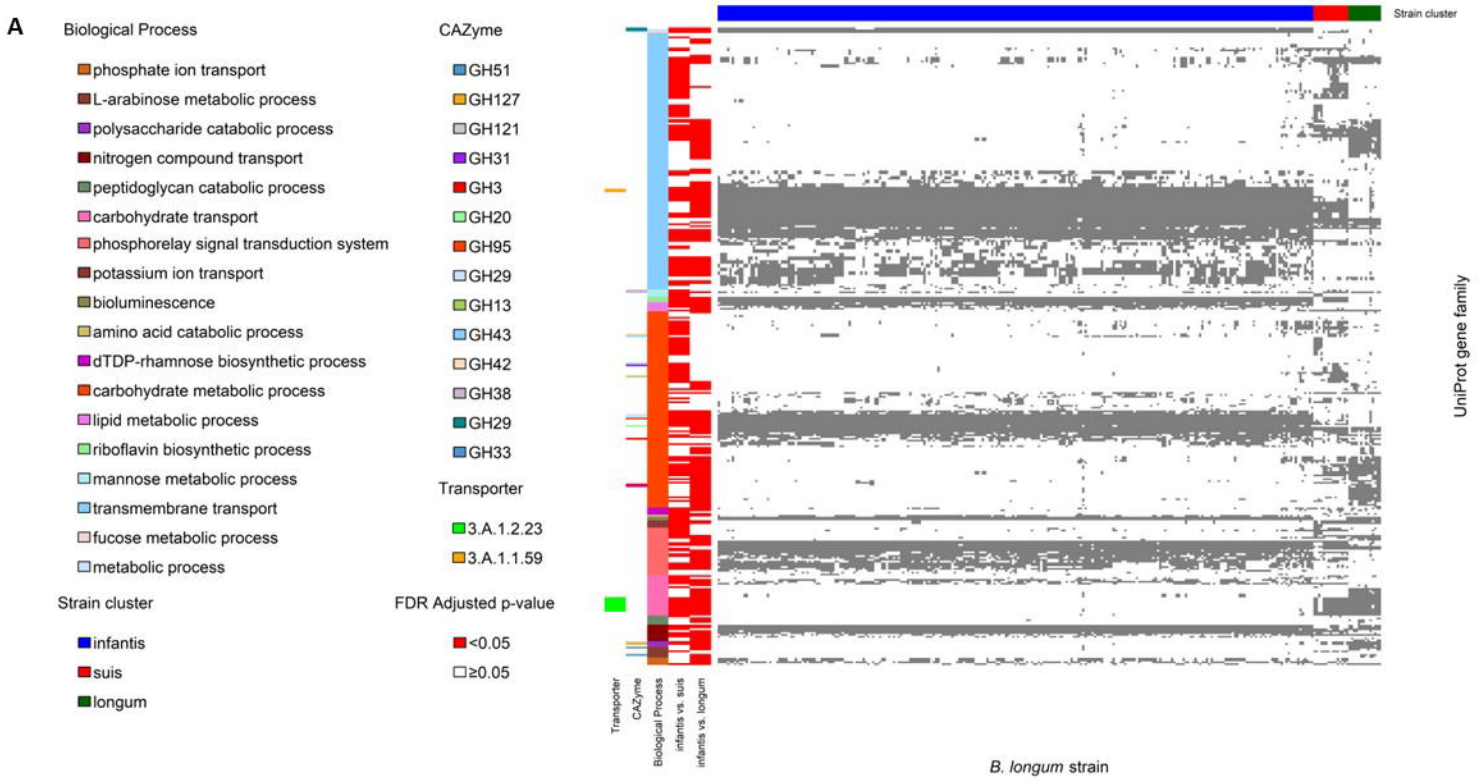

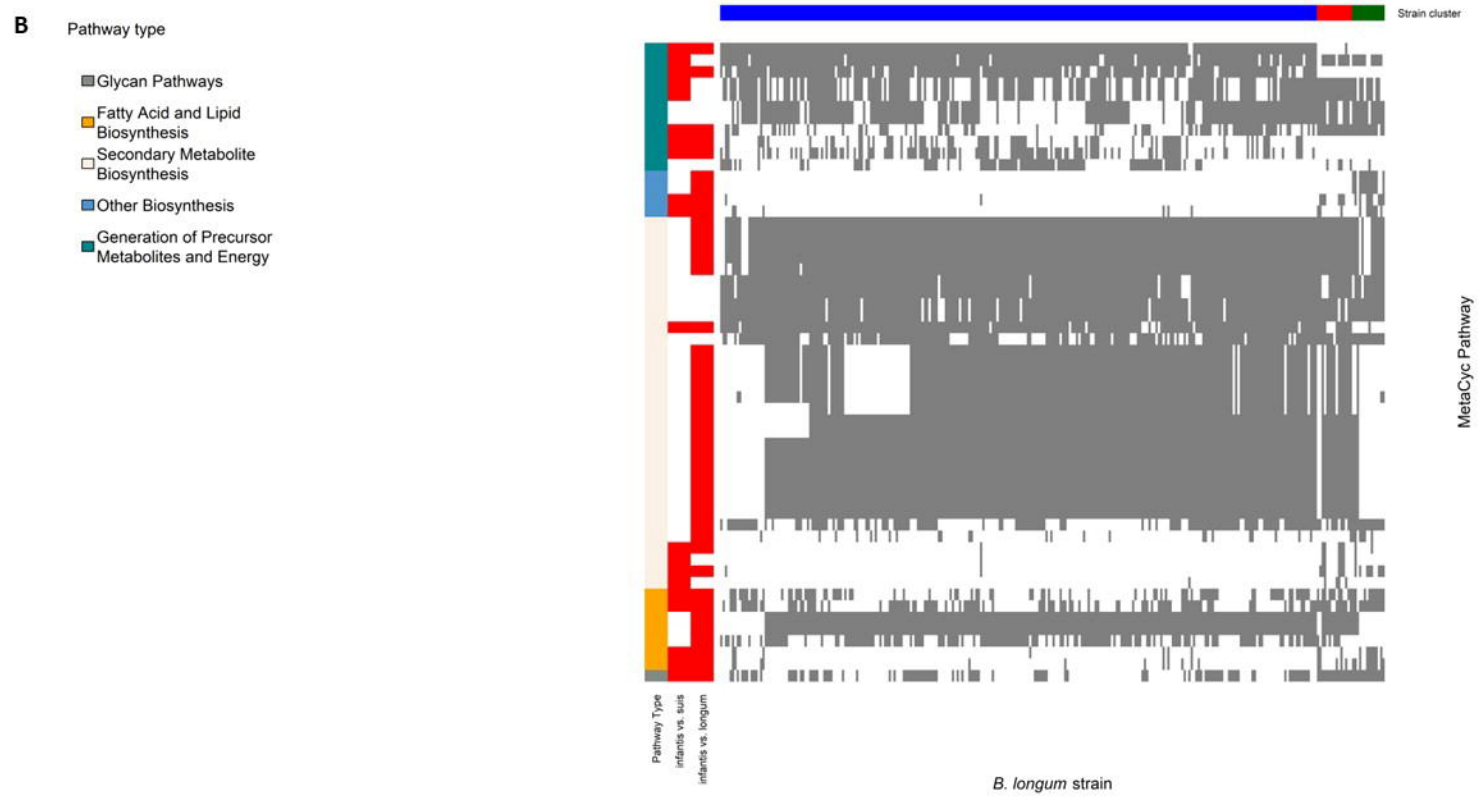

Table 1. Multivariable regression model[1] to estimate modification of IYCF on stunting at 18mo by mother-infant Lewis-null secretor phenotype discordance among 792 infants in whom mother and infant FUT2 and FUT3 status was ascertained

	Main Effect			Difference-in-Differences for IYCF by FUT2 and FUT3 phenotype combination		
	PD (95%CI)	**p-value**	**Adjusted p-value[2]**	**PD (95%CI)**	**p-value**	**Adjusted p-value[2]**
Both FUT2+/FUT3-	ref	ref	ref	ref	ref	
None FUT2+/FUT3-	0.13(0.01,0.25)	0.041	0.330	-0.21(-0.42,-0.01)	0.039	0.118
Infant only FUT2+/FUT3-	0.15(-0.03,0.33)	0.094	0.277	-0.21(-0.48,0.06)	0.127	0.191
Mom only FUT2+/FUT3-	0.29(0.14,0.44)	0.000	0.007	-0.33(-0.55,-0.10)	0.005	0.015
non-IYCF	ref	ref	ref			
IYCF	0.16(-0.02,0.35)	0.138	0.177			

[1]Covariates include season of birth, birthweight, infant sex, ever exclusive breastfeeding at 3mo, age at the 6mo visit, infant WHZ at the 6mo visit, and infant LAZ at the 6mo visit

[2]Adjusted for multiple hypothesis testing by the Benjamini-Hochberg method

PD, prevalence difference; 95%CI, 95% confidence interval; ref, referent

Table 2. Multivariable regression models[1] to estimate modification of IYCF on stunting at 18mo by infant gut microbiome species turnover in 53 infants

	PD(95%CI)	p-value	Adjusted p-value[2]
PCoA Axis 1		n/N=17/53	
IYCF	-0.51(-0.99,-0.12)	0.009	0.045
PC1	0.21(-0.99,0.45)	0.085	0.204
PC1-by-IYCF[3]	-0.76(-0.99,-0.32)	0.001	0.003
PCoA Axis 2		n/N=17/53	
IYCF	-0.14(-0.99,0.12)	0.293	0.469
PC2	-0.06(-0.99,-0.01)	0.020	0.068
PC2-by-IYCF[3]	0.14(0.07,0.21)	<0.001	0.001
PCoA Axis 3		n/N=17/53	
IYCF	0.09(-0.99,0.39)	0.543	0.686
PC3	0.04(-0.99,0.09)	0.156	0.340
PC3-by-IYCF[3]	-0.08(-0.99,-0.02)	0.016	0.032
PCoA Axis 4		n/N=17/53	
IYCF	0.03(-0.99,0.31)	0.847	0.924
PC4	0.00(-0.99,0.06)	0.994	0.994
PC4-by-IYCF[3]	0.03(-0.99,0.12)	0.438	0.501

[1]Covariates include birthweight, infant sex, age at the 6mo visit, infant LAZ at the 6mo visit, infant diet diveristy score at the 6mo visit, and mother-infant Lewis-null secretor phenotype discordance coded as both, none, infant only or mother only

[2]Adjusted for multiple hypothesis testing by the Benjamini-Hochberg method

[3]Differences-in-differences

PD, prevalence difference; 95%CI, 95% confidence interval

Table 3. Multivariable regression models[1] to estimate modification of IYCF on stunting at 18mo by infant gut microbiome species in 53 infants

	PD(95%CI)	p-value	Adjusted p-value[2]
Bifidobacterium longum		n/N=17/53	
IYCF	-0.16(-0.43,0.10)	0.232	0.976
B.longum	-0.24(-0.43,-0.05)	0.014	0.068
B.longum-by-IYCF[3]	0.50(0.26,0.74)	<0.001	<0.001
Bifidobacterium pseudocatenulatum		n/N=17/53	
IYCF	-0.54(-1.02,-0.06)	0.029	0.304
B.pseudocatenulatum	1.82(0.48,3.15)	0.008	0.051
B.pseudocatenulatum-by-IYCF[3]	-2.00(-3.33,-0.68)	0.003	0.014
Escherichia coli		n/N=17/53	
IYCF	0.04(-0.25,0.33)	0.774	1.000
E.coli	0.01(-0.10,0.13)	0.823	0.859
E.coli-by-IYCF[3]	-0.07(-0.21,0.08)	0.362	0.592
Dorea longicatena		n/N=17/53	
IYCF	0.02(-0.27,0.31)	0.896	1.000
D.longicatena	-0.02(-0.13,0.09)	0.725	0.859
D.longicatena-by-IYCF[3]	0.03(-0.39,0.44)	0.898	0.898
Dorea formicigenerans		n/N=17/53	
IYCF	-0.18(-0.37,0.01)	0.062	0.324
D.formicigenerans	-0.18(-0.33,-0.03)	0.018	0.073
D.formicigenerans-by-IYCF[3]	-0.50(-1.00,-0.00)	0.048	0.145

1Covariates include birthweight, infant sex, age at the 6mo visit, infant LAZ at the 6mo visit, infant diet diveristy score at the 6mo visit, and mother-infant Lewis-null secretor phenotype discordance coded as both, none, infant only or mother only

[2]Adjusted for multiple hypothesis testing by the Benjamini-Hochberg method

[3]Differences-in-differences

PD, prevalence difference; 95%CI, 95% confidence interval